DEVELOPMENT OF EXPERIMENTAL TEST SETUPS FOR BLADED DISKS AND NON-LINEAR VIBRATION

A THESIS SUBMITTED TO
THE GRADUATE SCHOOL OF NATURAL AND APPLIED SCIENCES
OF
MIDDLE EAST TECHNICAL UNIVERSITY

BY

EREN ÖNEY

IN PARTIAL FULFILLMENT OF THE REQUIREMENTS
FOR
THE DEGREE OF MASTER OF SCIENCE
IN
MECHANICAL ENGINEERING

DECEMBER 2019

Approval of the thesis:

DEVELOPMENT OF EXPERIMENTAL TEST SETUPS FOR BLADED DISKS AND NON-LINEAR VIBRATION

submitted by **EREN ÖNEY** in partial fulfillment of the requirements for the degree of **Master of Science in Mechanical Engineering Department, Middle East Technical University** by,

Prof. Dr. Halil Kalıpçılar
Dean, Graduate School of **Natural and Applied Sciences** ________________

Prof. Dr. Sahir Arıkan
Head of Department, **Mechanical Engineering** ________________

Prof. Dr. Ender Ciğeroğlu
Supervisor, **Mechanical Engineering, METU** ________________

Examining Committee Members:

Assoc. Prof. Dr. Yiğit Yazıcıoğlu
Mechanical Engineering Department, METU ________________

Prof. Dr. Ender Ciğeroğlu
Mechanical Engineering, METU ________________

Assist. Prof. Dr. Gökhan Özgen
Mechanical Engineering Department, METU ________________

Assist. Prof. Dr. Orkun Özşahin
Mechanical Engineering Department, METU ________________

Assist. Prof. Dr. Bülent İrfanoğlu
Department of Mechatronics Engineering, Atılım University ________________

Date: 04.12.2019

I hereby declare that all information in this document has been obtained and presented in accordance with academic rules and ethical conduct. I also declare that, as required by these rules and conduct, I have fully cited and referenced all material and results that are not original to this work.

Name, Surname: Eren Öney

Signature:

ABSTRACT

DEVELOPMENT OF EXPERIMENTAL TEST SETUPS FOR BLADED DISKS AND NON-LINEAR VIBRATION

Öney, Eren
Master of Science, Mechanical Engineering
Supervisor: Prof. Dr. Ender Ciğeroğlu

December 2019, 71 pages

High-cycle fatigue is one of the most frequent reason of failure for turbomachines and in early design process, so it is crucial to predict the vibration levels. Various finite element modelling techniques for bladed-disk systems appear in the literature, including both reducing large size FEM and describing the frictional contact interface. However, not only having a large size FEM but also including the nonlinear friction to models makes the task very struggling and time consuming. In order to enhance the working life, resonances should be avoided but, it is not easy to avoid all critical resonances on turbomachinery due to the broad spectrum of aerodynamic excitation. Thus, decreasing the vibration amplitudes become necessary. The vibration amplitudes of the system can be reduced by the initial gap and friction between the shroud contact interface which is a nonlinear contact phenomenon. Therefore, calculating the dynamic properties of system is a major problem. This study is conducted in order to understand the nonlinear frictional contact behavior and gap nonlinearity which affects the damping characteristics of the shrouded blades. To do so, two experimental test setups are developed. First one consists of a shrouded blade to measure dynamic responses of stationary shrouded blade with gap nonlinearity. The effects of different shroud contact angle, shroud positions along radial direction, initial gap and different excitation forces are investigated on the first bending mode of the

blade. In the second test, an under platform damper setup is prepared. The effect of friction and normal preload at the contact surface is investigated. During both tests, a modal shaker for excitation and a data acquisition system with accelerometers are used for measurement,

Keywords: Gap Nonlinearity, Friction Nonlinearity, Bladed Disk, Experimental Nonlinear Vibration, Under Platform Damper

ÖZ

KANATÇIKLI DİSKLER İÇİN DOĞRUSAL OLMAYAN TİTREŞİM DENEY TEST DÜZENEKLERİNİN GELİŞTİRİLMESİ

Öney, Eren
Yüksek Lisans, Makina Mühendisliği
Tez Danışmanı: Prof. Dr. Ender Ciğeroğlu

Aralık 2019, 71 sayfa

Yüksek devirli yorulma, türbinlerin erken tasarım sürecinin en sık görülen başarısızlık nedenlerinden biridir, bu nedenle tasarım öncesi titreşim seviyelerini tahmin etmek çok önemlidir. Kanatçıklı disk sistemleri için çeşitli sonlu eleman modelleme teknikleri, büyük boyutlu sistemlerin boyutunun azaltılması ve sürtünme ara yüzünün modellenmesi dahil literatürde yer almaktadır. Bununla birlikte, yalnızca büyük boyutlu bir modele sahip olmakla kalmayıp, aynı zamanda modellere doğrusal olmayan sürtünmeyi de dahil etmek, işi çok zorlu ve zaman alıcı hale getirir. Çalışma ömrünü arttırmak için rezonans bölgelerinden kaçınılmalıdır, ancak geniş frekans bandına sahip aerodinamik uyarma spektrumu nedeniyle turbo makinalarda tüm kritik rezonanslardan kaçınmak kolay değildir. Bundan dolayı, titreşim genliklerinin azaltılması gerekli hale gelir. Sistemin titreşim genlikleri, doğrusal olmayan temas arayüzü arasındaki ilk boşluk ve sürtünme ile azaltılabilir. Bu nedenle, sistemin dinamik özelliklerini hesaplamak büyük bir sorundur. Bu çalışma, kanatçıklı disklerin sönümleme özelliklerini etkileyen doğrusal olmayan sürtünmeli temas davranışını ve ilk aralık davranışını anlamak amacıyla yapılmıştır. Bunu yapmak için, iki deneysel test düzeneği geliştirilmiştir. Birincisi, sistemin doğrusal olmayan boşluk ile dinamik tepkilerini ölçmek için kanatlı bir bıçaktan oluşmaktadır. Bıçağın ilk bükülme modu

üzerinde farklı kanatçık temas açılarının, kanatçıkların radyal doğrultuda farklı konumlarının, başlangıç boşluğunun ve farklı uyarma kuvvetlerinin etkileri incelenmiştir. İkinci testte, platform altı sönümleyici test düzeneği kurulumu hazırlanmıştır. Temas yüzeyindeki sürtünme ve normal önyüklemenin etkisi incelenmiştir. Her iki test sırasında, uyarma için modal sarsıcı, ivmeölçer içeren bir veri toplama sistemi ölçüm için kullanılmıştır.

Anahtar Kelimeler: Aralık Doğrusalsızlığı, Doğrusal Olmayan Sürtünme, Kanatçıklı Disk, Deneysel Doğsural Olmayan Titreşim, Doğrusal Olmayan Titreşim Test Düzeneği, Platform Altı Sönümleyici

This thesis is dedicated to my whole college life and my beloved eternal friends who turned these years to a beautiful journey with unforgettable memories.

ACKNOWLEDGEMENTS

First and foremost, I thank my mother and father for their support in every aspect throughout my life.

I would like to express my gratitude to my thesis advisor Prof. Dr. Ender CİĞEROĞLU for his enormous effort, knowledge and encouragement on my thesis and vibration topics which affected my career.

I cannot think of a college life without my dear genius friends Mr. Hazim Sefa KIZILAY and Mr. Gökhan KARAPISTIK. I am grateful to know them and thank them deeply for all their supports throughout this thesis period.

I would like to thank my love Gözde for her support, patience and kindness in my rough times. Thanks to her I've found a reason in my life in every aspect.

I would like to thank my associates who enhanced my both practical and technical knowledge in vibration topics.

To all my beloved friends which I cannot listed in here, thank you for being by my side and your understanding and friendship.

TABLE OF CONTENTS

LIST OF TABLES

TABLES

LIST OF FIGURES

FIGURES

CHAPTER 1

INTRODUCTION

1.1. Overview

Turbomachinery bladed disks took attention of the researchers working in the field of structural dynamics in the past fifty years. Increasing demand to higher performance turbomachinery restricts the engineers from operating the system at safe regions and makes getting away from resonances almost impossible. As a result, excessively high vibration amplitudes acting on the bladed disks reduces the working life, increases the maintenance cost and even results in catastrophic failure of the structure due to the high cycle fatigue (HCF) [1]. Thus, in order to reduce the high amplitude vibration levels down to reasonable limits and increase the high cycle fatigue life of bladed disk systems, introducing friction to the system is a highly encountered solution. In this thesis, two different damping techniques which are shroud friction with gap and under platform damper are discussed.

1.2. Literature Survey

High amplitude vibration levels can be reduced down to reasonable limits and HCF life of bladed disk systems can be increased by introducing friction between the shroud contacts or under platform which are simple and effective ways. However, introducing friction contact to the system brings nonlinearity and in order to understand this behavior, frictional parameters must be accurately measured. To do so, several test rigs are developed to represent either the whole blade assembly or a section of it. In order to identify the model parameters accurately, Mainak Mitra et al. [2], developed a test rig which consists of a cantilever blade-like beam with floating contact under a normal load at the free end. They emphasized the importance of normal load distribution on the nonlinear system response in the case of large contacts and hence they parameterized the normal load distribution as a spatial function. Berruti et al. [3] developed a test rig in order to analyze the effect of frictional damping in laboratory with the original parts of the bladed segments of a turbine. Hence, the same assembly type which is used in service could be investigated in detail. In the study of D'Ambrosio [4] two different test rigs are constructed one of which consists of a single blade with a dry friction damper at the free end and the other contains 13 blades which is more complex. They analyzed the dry friction behavior in the first simple case and focused more on the dynamical behavior of the bladed disk connected by nonlinear elements on the complex test setup. More studies have been conducted on blades with friction dampers regarding the effect of damping on the structure response also by Griffin [5] and Szwedowicz [6]. However, the results are limited since there are more parameters affecting the performance of the shrouded blades such as shroud angle, preload between the shrouds and shroud position in radial axis which make the shroud analysis more complex. The ratio of the preload on the contact surface to the excitation force is one of the main parameters effecting the contact state. By adjusting this ratio three different contact states namely completely stuck, completely slip and stick/slip can be achieved [7]. Hence, controlling the excitation force is important in order to obtain good agreement with the numerical results with high accuracy. Other than that, the radial position of the shroud influences the dynamical response of the structure, so it should also be taken into account for optimized damping during the design stage. In the study of Kaptan et al. [8] the shrouded blade is fixed from the root and the normal load the contact interface is simulated by dead weights and the neighboring blades are simulated by high mass blocks. By changing the load at the contact interface different operational points of the turbine are represented. Since the main objective is to focus on the effect of normal load at the contact interface to the blade response, the effect of stiffening due to the rotational speed is neglected. Test results are compared with the numerical simulation results and a good agreement is obtained. Sanliturk et. al. [9] studied theoretical modeling and analysis of wedge-shaped under platform dampers for turbine blades. The main objective of their study is to reduce the number of experiments which is conducted to optimize damper parameters. Experimentally measured contact results are converted by using their theoretical model in order to utilize contact parameters in analysis of nonlinear structures with contact nonlinearity. Developed model for nonlinear vibration analysis is verified by comparing experimental results for two different test setups. In the first test setup, cantilever beams are investigated to simulate contact friction nonlinearity in sector of a bladed disk with under platform damper. In the second test setup, real turbine blades with real under platform damper are studied by comparing the result of theoretical model. They conclude that proposed analysis method is applicable to obtain nonlinear characteristics of structures with under platform damper. Also, they suggest that empirical data has to be corrected in order to obtain more accurate theoretical results. Sever [10] studied on a test setup for rotating bladed disk with full set of under platform dampers in realistic rotating condition. A new method to collect reliable data by using laser doppler vibrometers (LDV) from rotating test ring which is constructed for experiment is proposed and explained. In force response analysis process, a single bladed sector is modelled and then cyclic symmetric approach is applied to obtain full model vibration characteristics. In order to transform equation of motion of the structure to algebraic nonlinear equation set, multi harmonic balance method is utilized. They claim that effect of contact stiffness on response curve is less than effect of friction coefficient and found that response obtained from analysis and measurement data have good agreement. Firrone [11] studied on kinematics of two different under platforms which are tested for deflection shapes and dynamic response of the structure. Novelty of the study comes from use of laser doppler vibrometers to measure the damper displacements. Displacements obtained from test and numerical analysis are compared for design of under platform damper. In phase and out of phase mode of a bladed disk sector with two different under platform damper are investigated experimentally. Cylindrical and wedge damper configurations are tested. Semenova et. al. [12] studied on under-platform damper for gas turbine blades. Model reduction method based on Craig-Bampton and Guyan method is presented. In order to verify the proposed method, experimental study is conducted by using special test rig, shaker and laser vibrometer. Vibration displacement amplitude of blades is investigated for different centrifugal loads. In and out of phase modes of blades are studied experimentally to explore effect of the under platform damper on blade vibration. In Botto and Umer's study [13], a novel experimental test setup is designed which is aimed to investigate the under platform damper dynamics in detail. Instead of evaluating the performance of under platform dampers on overall blade response, they are more focused on damper kinematics by measuring damper displacement and contact forces. Designed test setup consists of a single blade clamped at the dovetail root with a specific clamping mechanism and two under platform dampers on both sides of the blade. The contact forces at the interface are measured with loadcells placed at free ends of the dampers. In the study of Pesaresi [14], the effect of surface roughness at the contact interface is investigated in detail. In order to minimize the effect of external frictional factors, they used a wire cut single block with a blade on it. The two bladed blocks are clamped with a hydraulic cylinder to ensure a fixed boundary. A wedge type under platform damper is used during the tests and the normal load is simulated by a pulley system with dead weights hanged. They also utilized a noncontact measurement system LDV to measure the blade tip displacements. Their new modelling approach is evaluated with the experimental study which discretize the contact interface with 3D microslip contact elements. With their proposed method, the effect of microlevel contact behavior is also included in the simulations.

1.3. Objective of Thesis

Compared to the number of theoretical investigations on damping in bladed disks, experimental studies for characterization of nonlinear damping are quite low. This is mainly due to the difficulties related to measurement and excitation system as well as the need for carefully designed test setups. Moreover, involving nonlinear elements like friction damper or initial gap to the system complicates the task even more. The modification effects caused by the instrumentation itself shall also be included during design stage of the test setups.

There are two main objectives of this thesis first of which is to design an experimental shrouded blade test setup to investigate the damping characteristics of friction and gap nonlinearity for several design alternatives and secondly, to design an experimental under platform test setup to investigate the effect of friction on vibration amplitudes during different phases of the blades with different contact forces.

1.4. Outline of Thesis

Aim of this thesis is to provide a guideline for the non-linear experimental analysis and provide improvements on the design accordingly. In Chapter 2, an experimental test setup design process is explained which is used to analyze the friction and gap non-linearity effects on shrouded blade performance. In Chapter 3, a different test bench is designed to analyze another blade damping method which utilizes an under platform damper to reduce excessive vibration amplitudes. Results of both shrouded blade and under platform damper setups are presented in Chapter 4. Finally, in Chapter 5, conclusions about the non-linear damping behavior and possible improvements on the test platforms are discussed.

CHAPTER 2

DESIGN OF EXPERIMENTAL TEST SETUP FOR ANALYSIS OF GAP NONLINEARITY ON SHROUDED BLADES

2.1. Overview

This chapter concentrates on design and instrumentation of test setup for shrouded blade in detail. The designed shrouded blade test setup for investigating the effect of gap and friction nonlinearities is explained. Design constraints and considerations are stated to analyze the nonlinear effects efficiently. Afterwards, detailed information about the excitation and measurement system are introduced.

2.2. Design Constraints

In real turbomachinery systems, shroud surfaces get in contact due to the centrifugal force. This results in dissipation of energy due to friction and hence vibration amplitudes reduce significantly. Shroud angle, shroud position, excitation force and initial gap affects the dissipation amount and effect of these parameters can be investigated on the experimental tests easily. Moreover, experimental results provide improvements on analytical models. There are many restrictions in experimental testing which affects the final geometry and dynamics of the test setup. The general limitations can be listed as the available equipment, application of boundary conditions, maximum and minimum excitation amplitude, drivable frequency range, total weight, producibility etc. However, main restrictions for experimental vibration testing are excitation system capacity and available measurement system. Additional parameters shall be considered such as total weight, producibility etc. in order to conduct the tests efficiently.

For the shrouded blade test setup, shroud angles, alternative shroud positions, excitation point, amount of initial gap are also limiting factors for the geometry. These factors shall be considered well before the design in order to minimize external factors which may bring unwanted disturbances to the measurement.

2.3. Design of Shrouded Blade Test Setup

The experimental test setup CAD model and manufactured setup are shown in Figure 2.1 and Figure 2.2, respectively. The setup consists of 6 main components which are the blade, shrouds, blade base, shroud fixture, electrodynamic modal shaker and accelerometers. The blade (4) is mounted to the fixed base (1) and excited with a modal shaker (3). There are two types of shrouds (5) which have different contact angles and they are interchangeable at three different heights on both the blade and the shroud fixture (2). Excitation force is measured through the impedance head sensor fixed on the push rod and blade tip response is measured with a triaxial accelerometer (6).

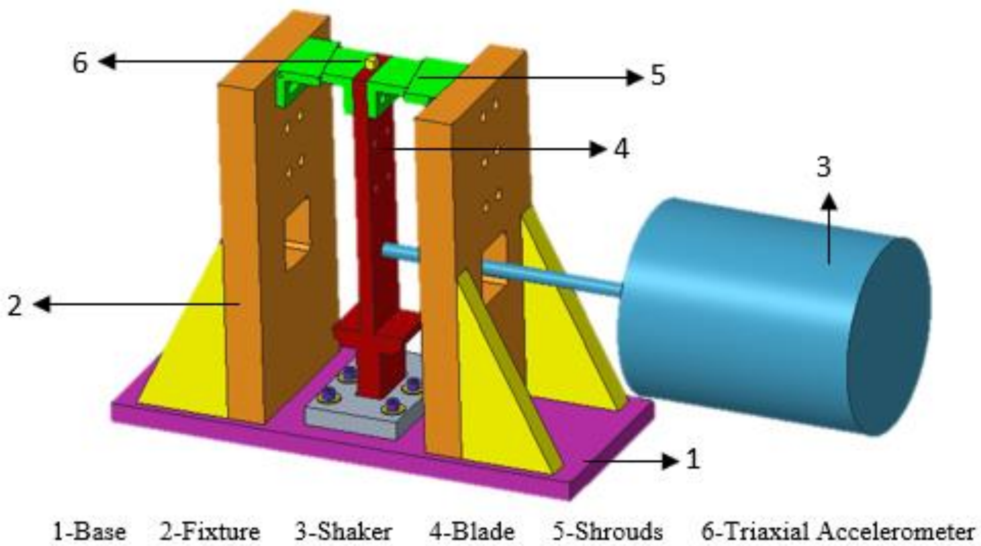

Figure 2.1. CAD Model of the Shrouded Blade Test Setup

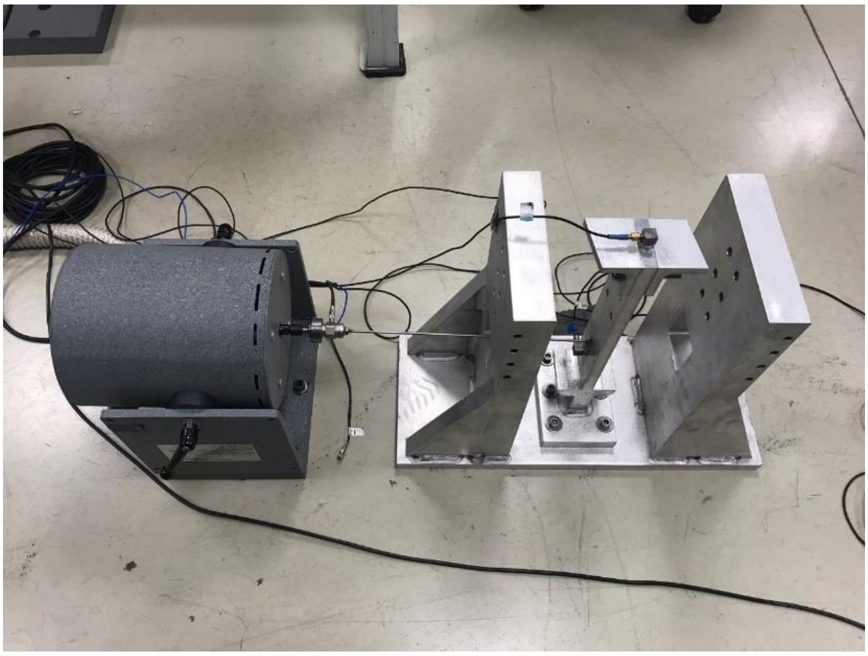

Figure 2.2. Experimental Shrouded Blade Test Setup

There are two types of shrouds with different shroud angles which are 10° and 30°. These shrouds can be positioned on the blade at three different heights. Moreover, in order to inspect the effect of the gap nonlinearity, four different initial gap distances which are 2mm, 1.5mm, 1.2mm and 1mm are selected. While changing the initial gap amounts, blade excitation force is kept constant at 40 N by sweeping the interested frequency range 30 – 200 Hz which covers the first free bending mode of the blade system. As a result, a total of 16 test scenarios are obtained and in order to eliminate the experimental errors, each test is conducted three times.

Normal load between the shroud interface results from the centrifugal force acting on the blade during operation. The effect of friction and gap during the operation is simulated by changing the amount of initial gap.

2.3.1. Finite Element Analysis of Shrouded Blade Test Setup

During the blade design, first bending natural frequencies of both the blade and the fixture are analyzed via ABAQUS software. The fixture is designed to be stiff enough to sustain the sliding behavior at the contact interface compared to the blade stiffness. After some iterations, blade and fixture geometries are tuned and final dimensions are obtained. Natural frequencies of the shrouded blade and fixtures are obtained by modal analysis. Modal analysis results of the final design are given in Table 2.1. Corresponding mode shapes of both blade and the fixture for different shroud positions are also shown in Figure 2.3, Figure 2.4 and Figure 2.5 respectively.

Table 2.1. *Modal Analysis Results of the Shrouded Blade and Fixture for Different Shroud Positions*

Natural Frequencies [Hz]			
	Shroud Position		
Mode #	**Top**	**Middle**	**Bottom**
Blade Mode 1	57.4	66.5	77.1
Blade Mode 2	278.6	314.1	353.2
Blade Mode 3	437.7	478.3	536.2
Fixture Mode 1	416.0	426.5	435.6

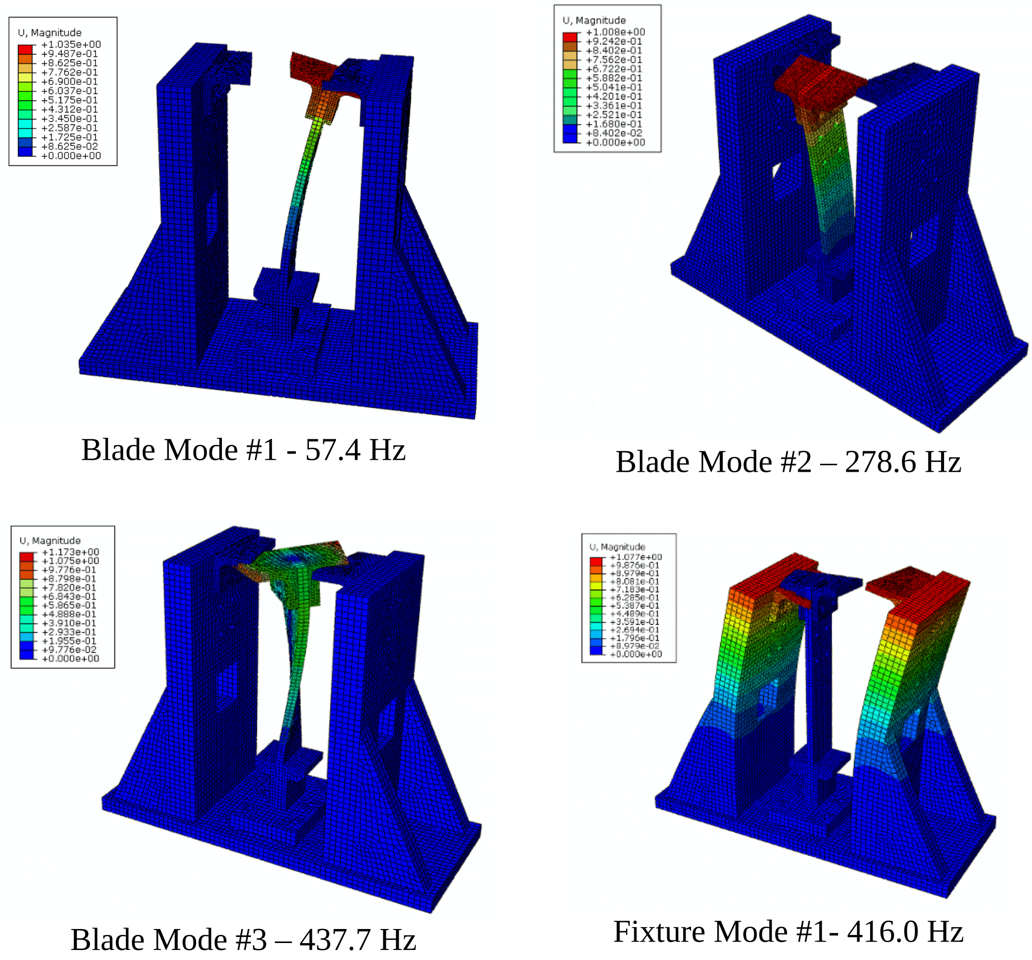

Figure 2.3. Mode Shapes of the Blade and Fixture with Shroud at Top

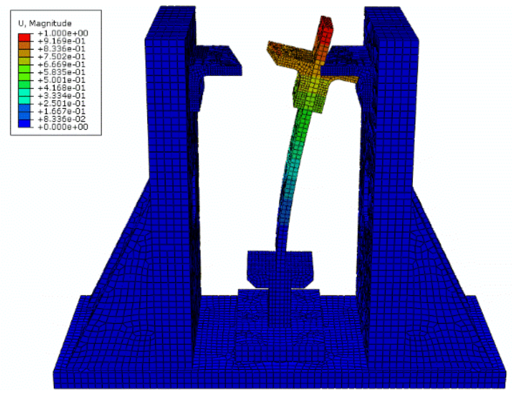

Blade Mode #1 – 66.5 Hz

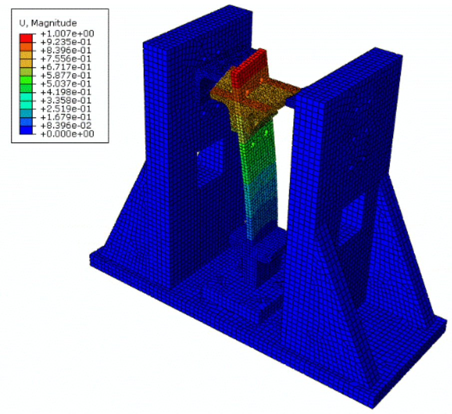

Blade Mode #2 – 314.1 Hz

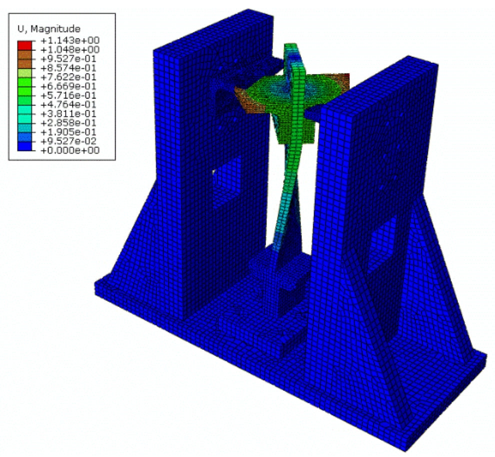

Blade Mode #3 – 478.3 Hz

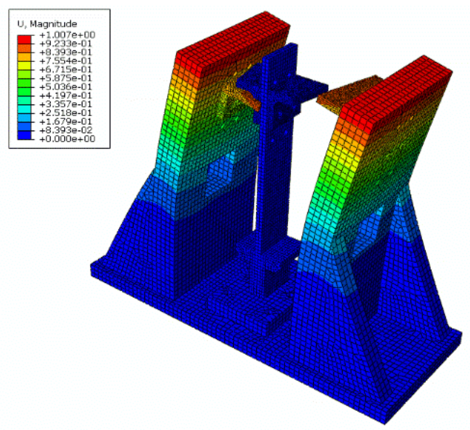

Fixture Mode #1- 426.5 Hz

Figure 2.4. Mode Shapes of the Blade and Fixture with Shroud at Middle

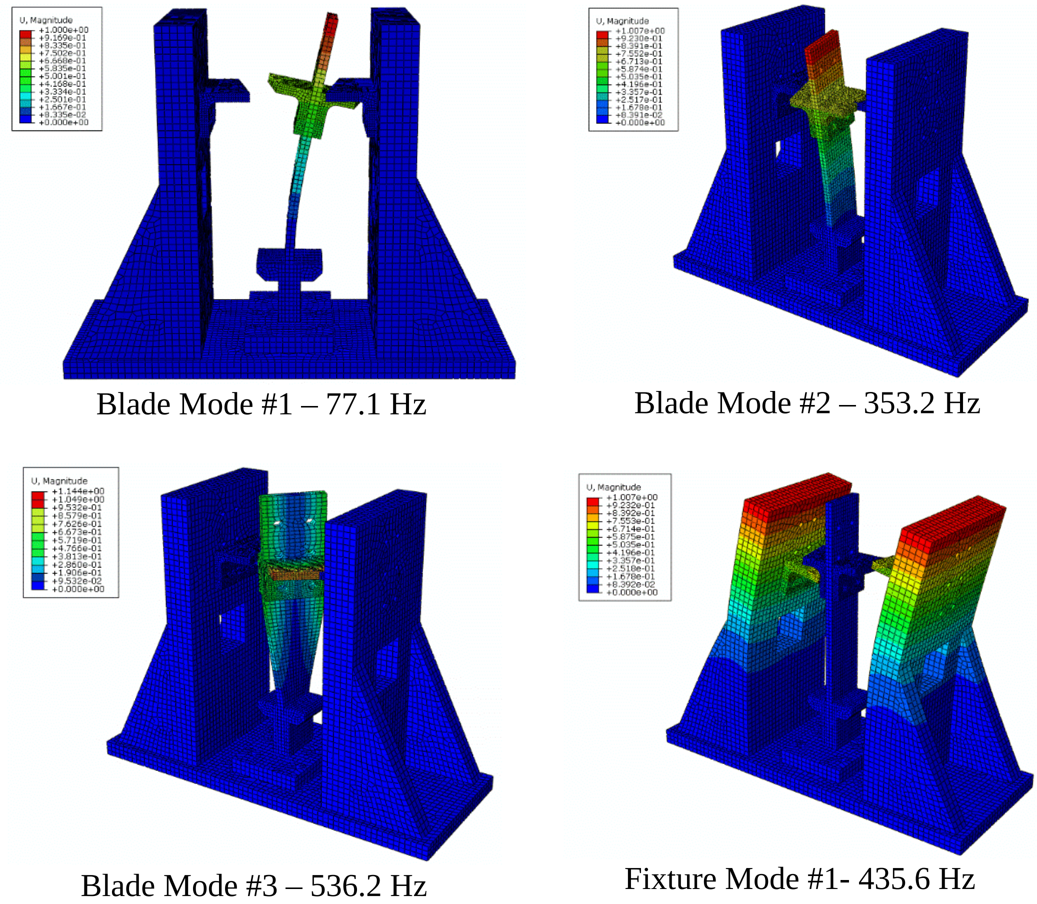

Figure 2.5. Mode Shapes of the Blade and Fixture with Shroud at Bottom

After the modal analysis, harmonic analysis is performed in order to analyze the tip point displacement FRF. The blade is excited from the exact same location with the test excitation point which is 170mm above the base plate upper surface. Response point is selected as the tip point of the blade since the maximum displacement occurs at the tip point. Excitation and response points are also shown in Figure 2.6

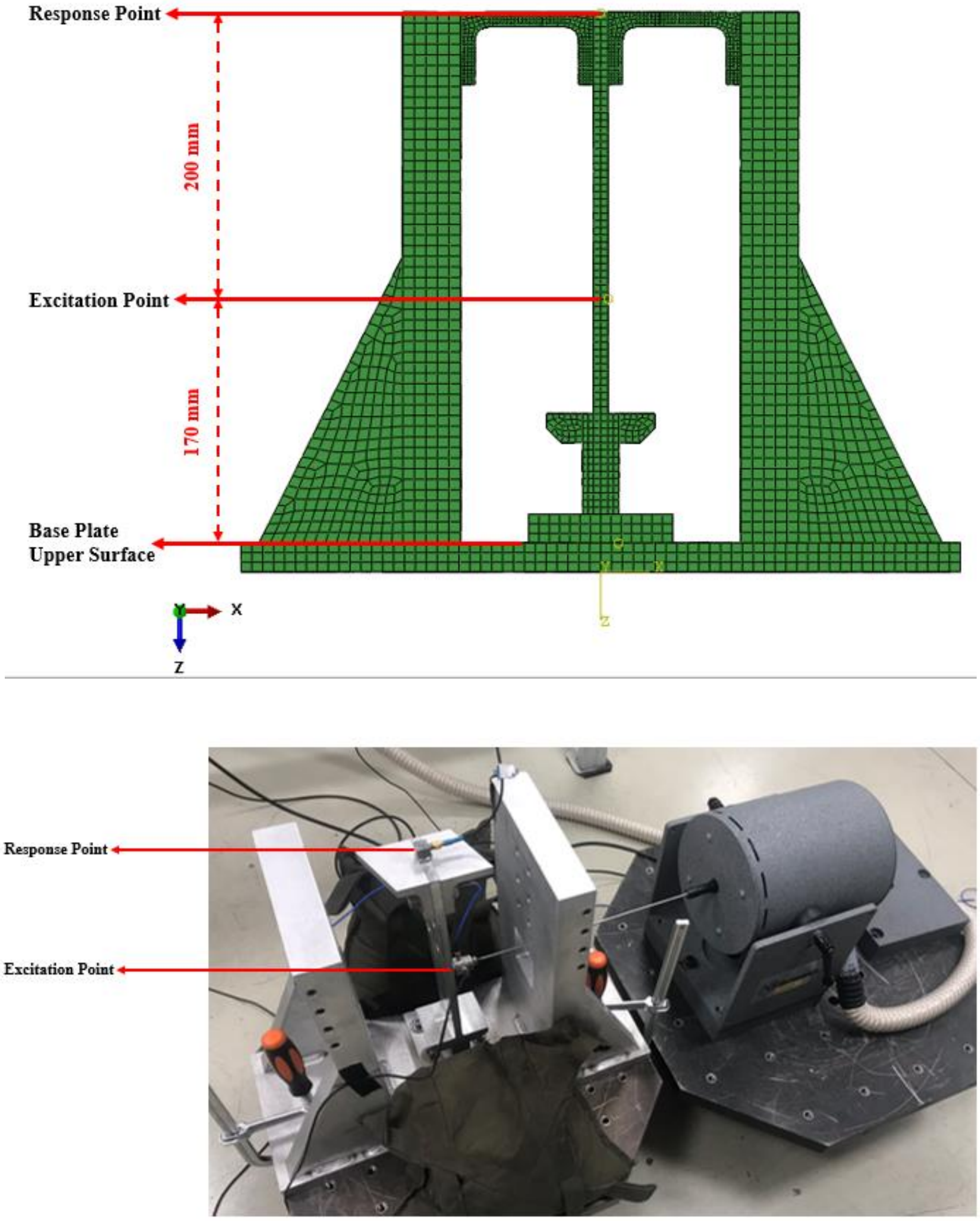

Figure 2.6. Excitation and Response Points - a) FEM, b) Experimental Setup

2.3.2. Shroud Design

Shroud angle and positions determine the width and length of the test setup. Depending on the contact angle, distance between the adjacent fixture and total length changes. Definition of the shroud contact angle is shown in Figure 2.7 for 10° shroud and 30° shroud is presented in Figure 2.8.

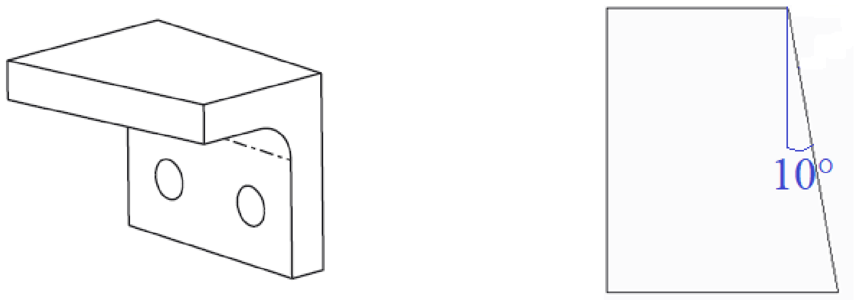

(a) (b)

Figure 2.7. Isometric (a) and Top View (b) of the 10° Shroud

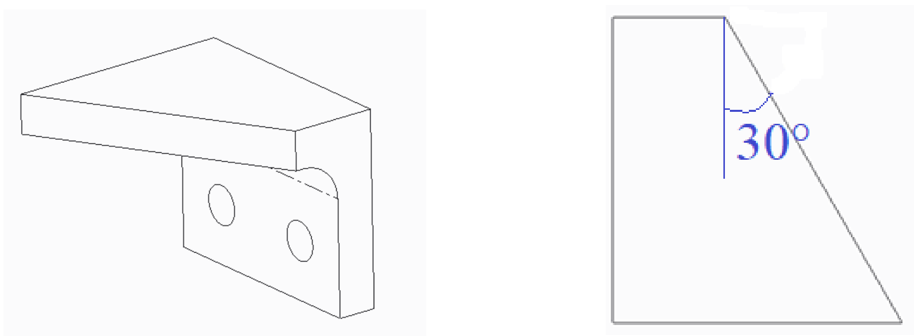

(a) (b)

Figure 2.8. Isometric (a) and Top View (b) of the 30° Shroud

As the shroud angle increases, the width and the distance between the blade and fixture increases. This issue effects the final geometry and hence it is important to determine the shroud angles before the production phase. After determining the angles, the setup geometries can be finalized.

2.4. Excitation and Measurement System

Excitation system consists of a computer, controller, power amplifier and a modal shaker. The main restriction comes from the modal shaker. It has a certain force output, maximum stroke and frequency range. During the tests, MB Dynamics Modal 50A shaker is used as exciter. For the low frequency excitation, the maximum stroke which is 25.4mm is the limitation since high displacements occur at low frequencies. Therefore, excitation point should be selected such that displacements will be below the maximum stroke and creates the desired displacement at the measurement point. In order not to push the limits of the exciter, 40N of constant excitation force applied which is adequate for obtaining desired displacements at the contact point. At the excitation point, DYTRAN Model 5860B impedance head is attached to the push rod or namely stinger in order to apply a constant force. The main objective of the push rod is to apply the controlled excitation to the structure in a desired direction. The force output from the impedance head is given to the VR8500 model vibration controller in order to apply a constant force over the interested frequency range. Input signal is generated by the controller and given to the MB500VI power amplifier which drives the modal shaker.

Measurement system consists of 500g range triaxial Kistler 8763B ICP type accelerometer. There occur high shock amplitudes during the impact, so in order to select the correct range initial tests should be conducted. LMS SCADAS Mobile data acquisition system is used for acceleration recordings and the sampling rate is adjusted to 16384 samples per second. As a rule of thumb, in order to gather correct amplitudes at least 10 times of the maximum interested frequency should be used. Anti-aliasing filtering is applied during the measurements.

Complete excitation and measurement system are shown schematically in Figure 2.9.

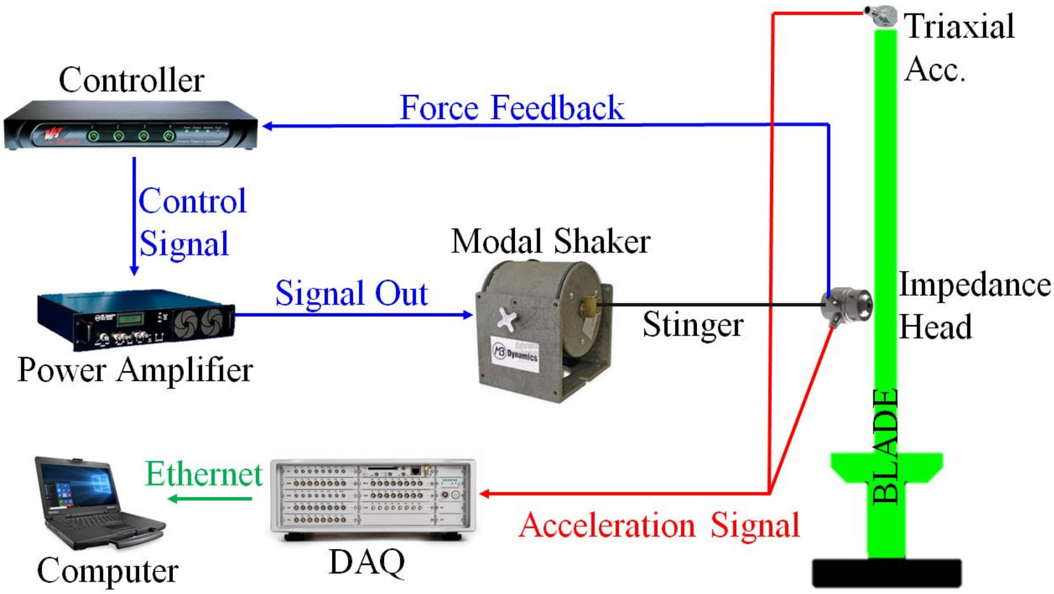

Figure 2.9. Excitation and Measurement System for Shrouded Blade Test Setup

2.5. Calculation of Displacement Frequency Response Function (FRF)

The tip point acceleration response is measured with an accelerometer and excitation force is measured with the impedance head during the tests. After measuring these quantities, the frequency response function is calculated through post processing.

Basically, frequency response function describes the relationship between the input and output of a system in frequency domain. Therefore, the input and output signals are converted to frequency domain by using Fast Fourier Transform (FFT) algorithm and then the acceleration signal is integrated twice to obtain the displacement. Finally, by dividing the displacement signal with the input force in the frequency domain, the displacement FRF, i.e. receptance is obtained. The schematic which covers the entire calculation step is given in Figure 2.10.

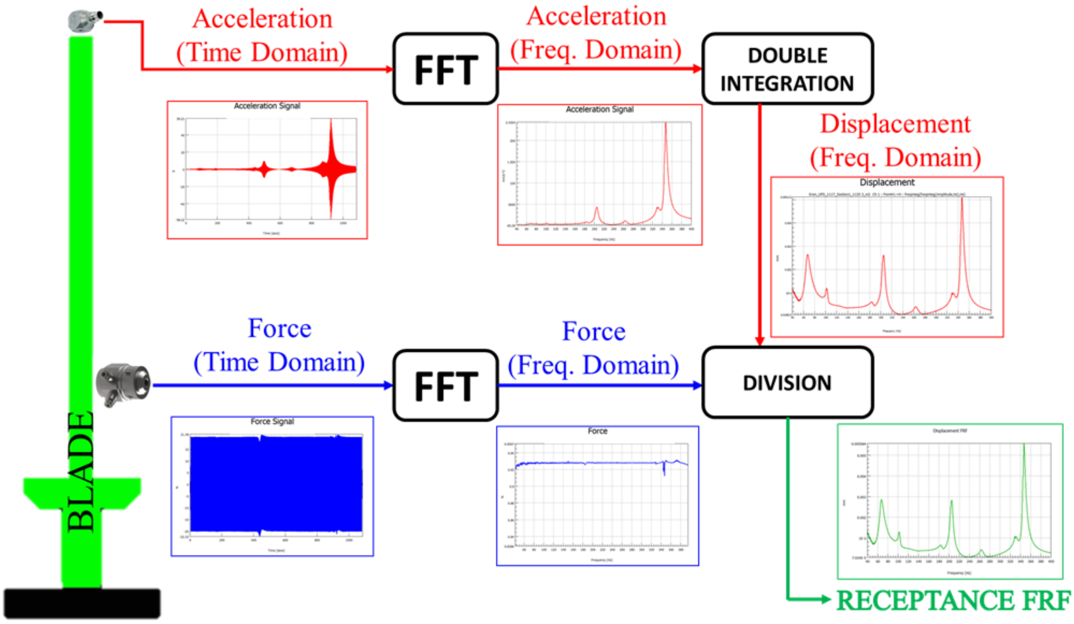

Figure 2.10. Calculation of Receptance (Displacement FRF)

2.6. Alternative Shrouded Blade Test Setup Design

After conducting several tests with the experimental shrouded blade test setup, some deductions are made which can be used to improve the current test setup for better understanding of the real bladed disk assembly.

First of all, the first test setup was designed for understanding the nonlinear gap and frictional behavior and in order to decouple the modal effects of the adjacent blades the fixtures are designed to be stiffer than the blade. Moreover, the effect of gap could be activated easily due to the high stiffness of the adjacent fixtures.

As an alternative, another test fixture is designed which is aimed to reflect the realistic bladed disk dynamical behavior. To do so, the fixtures' stiffnesses are reduced by reducing the thickness and trying to adjust it such that the first bending mode natural frequency is close to that of the blade. New setup is shown in Figure 2.11.

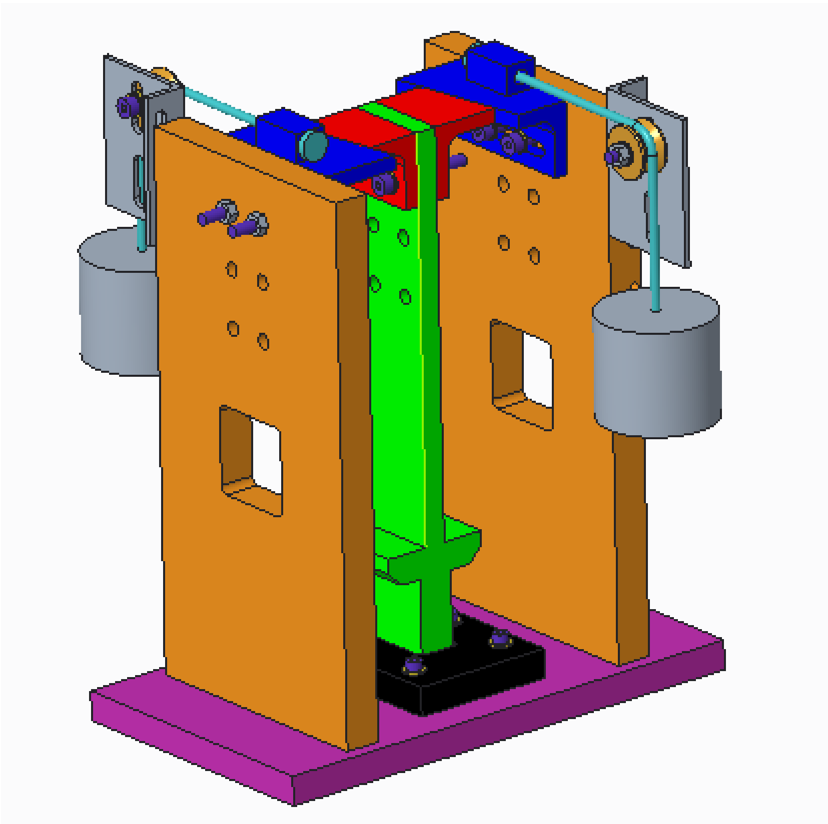

Figure 2.11. Alternative Bladed Disk Test Setup Design

Alternative design also contains a normal load application method which is aimed to create the effect of centrifugal force by dead weights. By applying different preloads at the contact interface different rotation speeds can be simulated and the nonlinear frictional behavior can be observed.

In order to determine the thickness of the fixtures several iterations are made with ABAQUS modal analysis. Finally, the thickness is determined as 15mm and the resulting modal properties are presented in

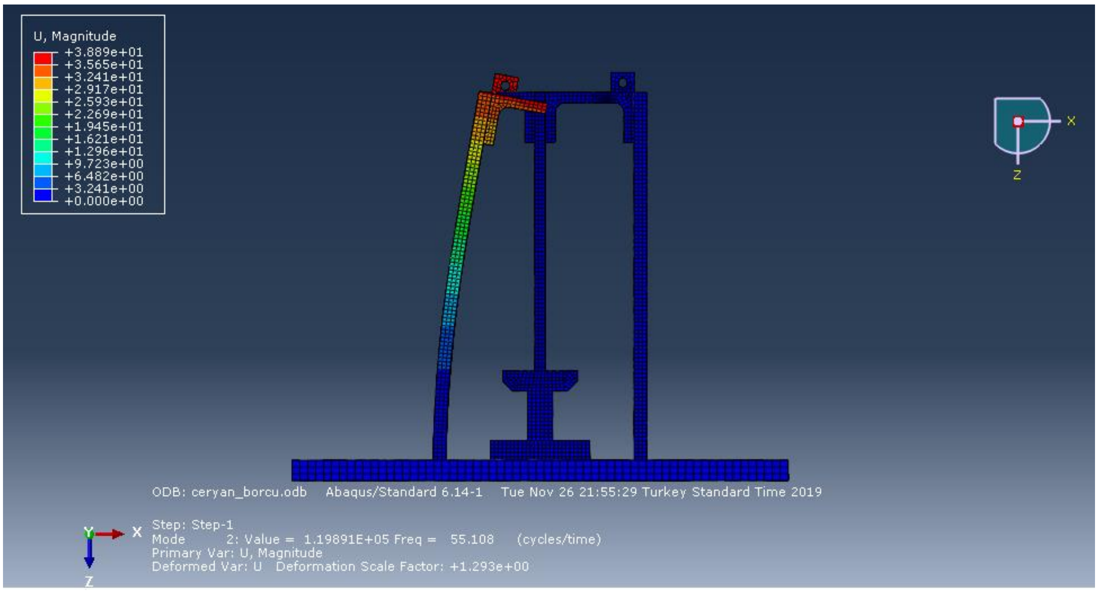

Figure 2.12. Modal Analysis of Alternative Test Setup

The fixture’s first bending mode natural frequency is adjusted to 55.1 Hz where the blade first bending natural frequency is 57.4 Hz.

CHAPTER 3

DESIGN OF EXPERIMENTAL TEST SETUP FOR UNDER PLATFORM DAMPER

3.1. Overview

In the turbine engine industry, under platform dampers are generally triangular shaped metal parts and they are put inside a cavity under the blade airfoils which allows the damper to move freely. When the engine starts rotating, the centrifugal force presses the under platform damper to the contact surface. Since the damper is free to move, due to the gas flow and vibrations relative motion occurs at the contact interface. Eventually, this results in frictional dissipation which reduces vibration amplitudes. In this chapter a simple UPD test rig development will be addressed and the challenges during the tests and improvements on the test setup will be discussed.

3.2. Design Constraints

In order to evaluate the dynamical behavior of an UPD correctly, it is important to obtain reliable test results from a controlled test setup. Identification parameters of UPD for analysis requires careful testing for validation of the analysis model.

For the under platform damper test setup, main limiting factor is the applicable normal load at the contact interface. In order to ensure a good conformity at the interface, the normal load the interface should be adjusted well. Also, the excitation force plays an important role together with the normal load. The ratio of the normal load to excitation force determines whether the damper slips or separates from the contact surface.

3.3. Design of Under Platform Damper Test Setup

During the design, similar constraints with the shrouded blade test setup are considered. Again, as the exciter MB Dynamics Modal 50A shaker is used together with LMS SCADAS Mobile data acquisition system. However, contrary to high acceleration amplitudes which occur in gap nonlinearity due to impact, friction nonlinearity has smoother behavior. Therefore, in UPD tests lower range accelerometers are used in order to increase the amplitude sensitivity of the measurements. Blade contact surfaces are placed to a certain height in order to access to the UPD easily. Also, to excite the system in the available frequency range blade geometry is tuned by considering the modal analysis results. Moreover, the normal load application consists of a leverage system.

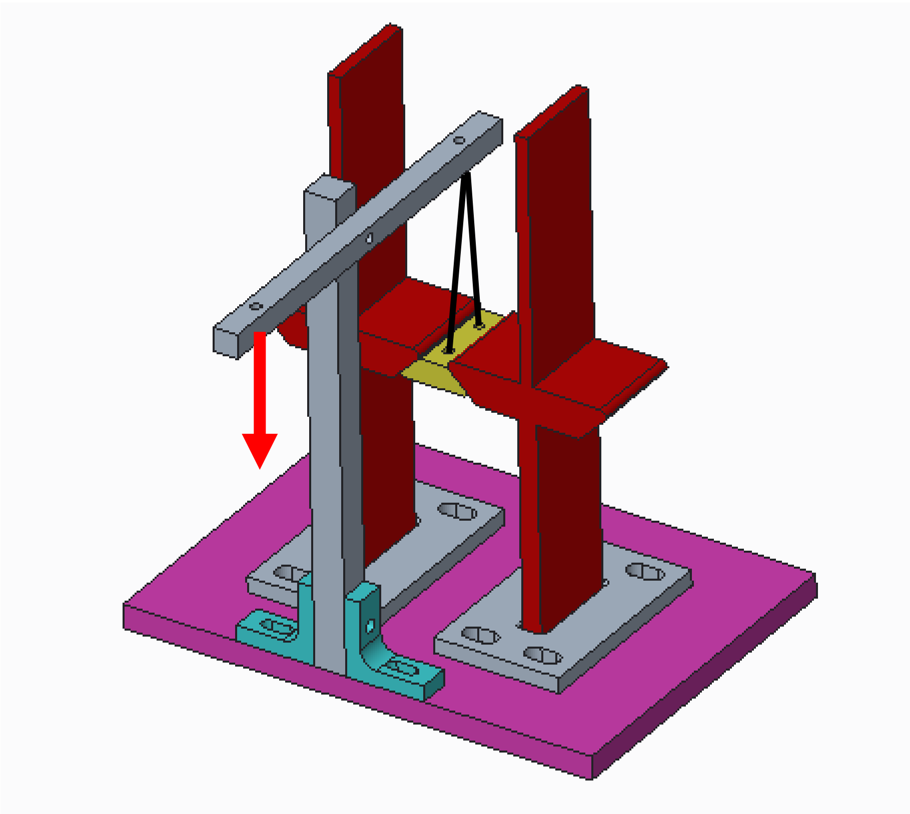

Figure 3.1. Under Platform Damper Test Rig CAD Model

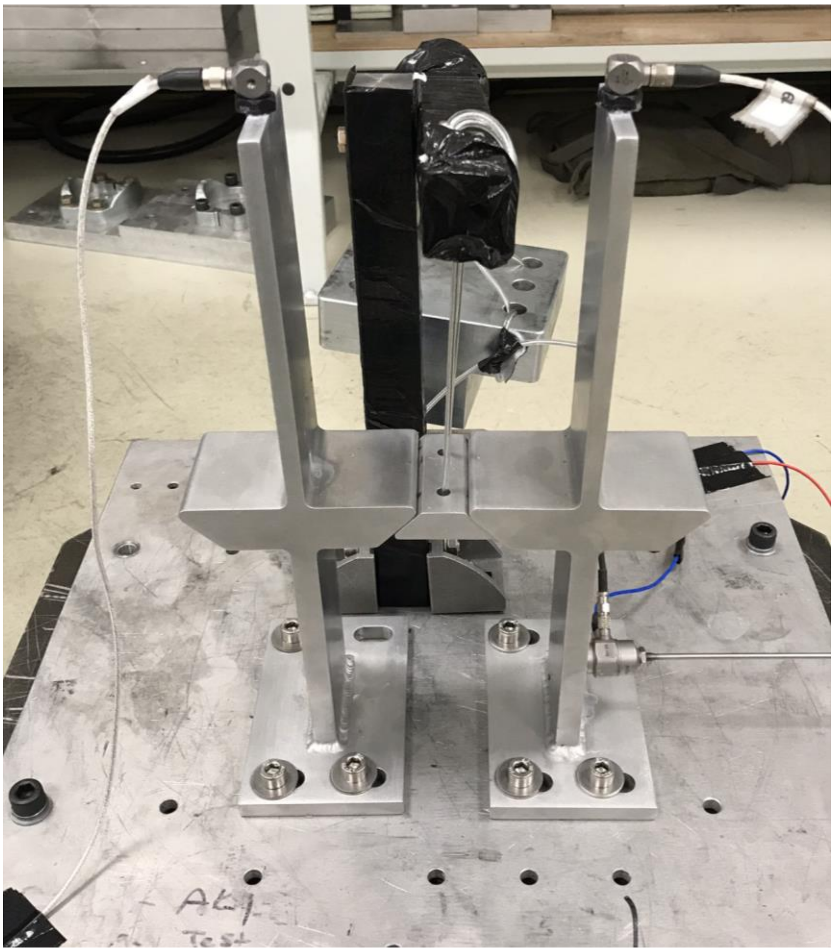

Figure 3.2. Under Platform Damper Test Rig Experimental Test Setup

3.3.1. UPD Blade Design

In order to determine the geometry of the blade, modal analysis is performed via ABAQUS. Modal analysis results are shown in Figure 3.3.

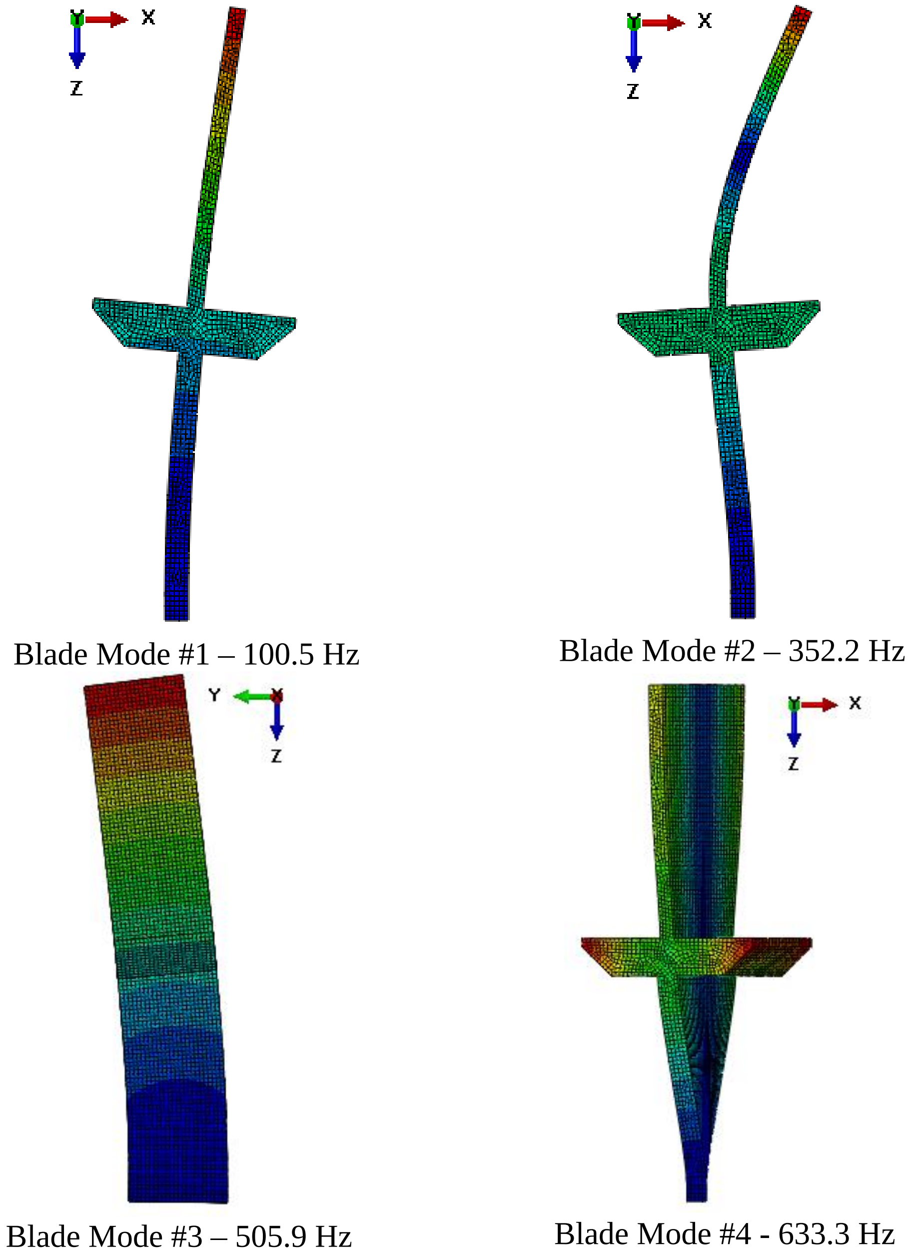

Blade Mode #1 – 100.5 Hz

Blade Mode #2 – 352.2 Hz

Blade Mode #3 – 505.9 Hz

Blade Mode #4 - 633.3 Hz

Figure 3.3. Modal Analysis Results of the UPD Blade

First bending mode of the blade is obtained as 100.5 Hz which is in the required frequency range for the shaker. When the blades coupled through the under platform damper, two important vibration modes occur which are called in-phase (IP) and out of phase (OoP) modes. For the experimental UPD setup with two blades, when the phase angle between two blades are 0°, they are called in-phase and when the phase angle is 180°, they are called out of phase. IP and OoP modes are shown schematically in Figure 3.4 and Figure 3.5, respectively.

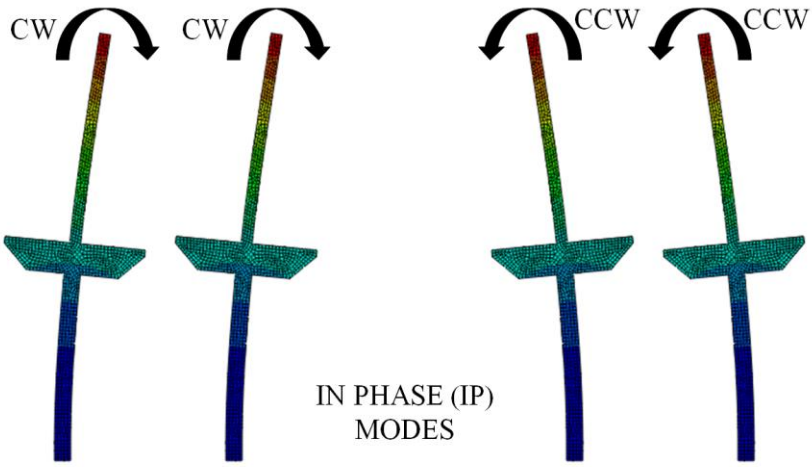

Figure 3.4. In Phase (IP) Vibration Modes

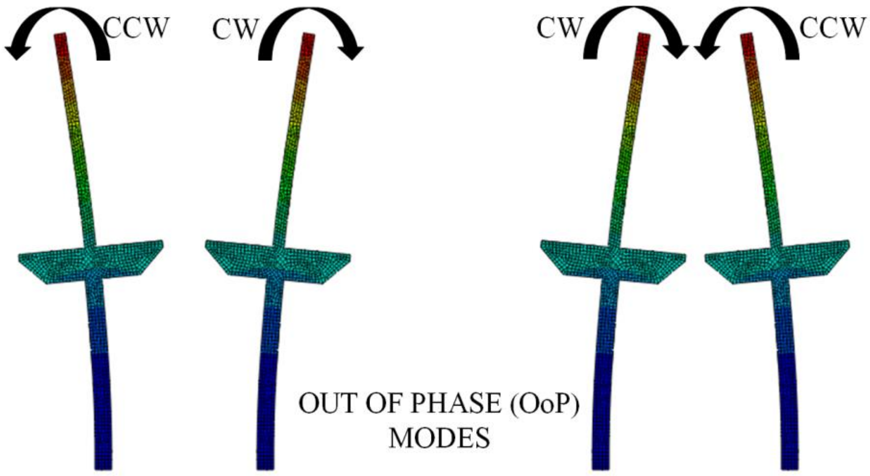

Figure 3.5. Out of Phase (OoP) Vibration Modes

3.3.2. Under Platform Damper Design

It is possible to design vast variety of UPD geometries and each of which will have a different damping characteristic. Symmetric, asymmetric and circular geometries are possible alternatives. Wedge dampers which have triangular cross section are most commonly used dampers in the literature. Moreover, there are asymmetrical wedge dampers which have different angles at each contact side. However, in order to apply equally distributed normal load at the contact interface, symmetrical wedge shaped UPD is selected for thesis. The contact surfaces have 45° inclination on both sides which enables tangential relative displacement on the contact surface. The designed wedge shaped UPD which has a triangular cross section with 45° contact angle is shown in Figure 3.6

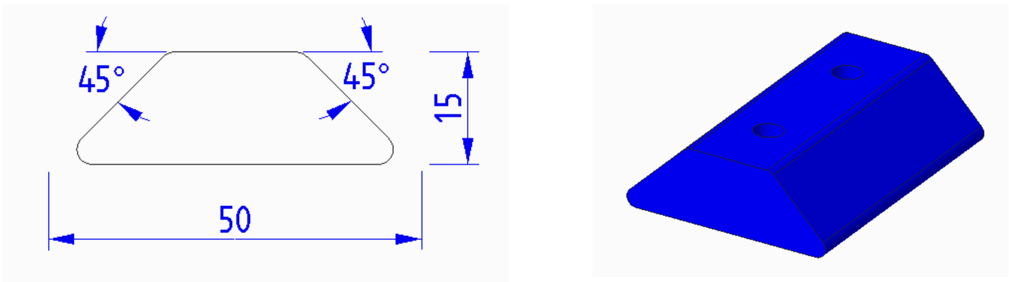

Figure 3.6. 45° Under Platform Damper Geometry (Dimensions in mm)

There are two holes in the designed UPD. In order to apply the normal preload, an inelastic cord is passed through these holes. Detailed information about the normal load application is given in the following section.

3.3.3. Application of Normal Load

The main challenge in UPD test setup design is to simulate the normal load between the UPD and blade contact surfaces which occurs due to the centrifugal force in real case. Two steel square cross section beams are manufactured for the normal load application. There are two inelastic cords passing through the UPD which is connected to the leverage system at one point. The leverage arm has a pin at the middle which allows rotation and by hanging a dead weight to the other end, normal load can be controlled. Normal load application can be seen at Figure 3.7

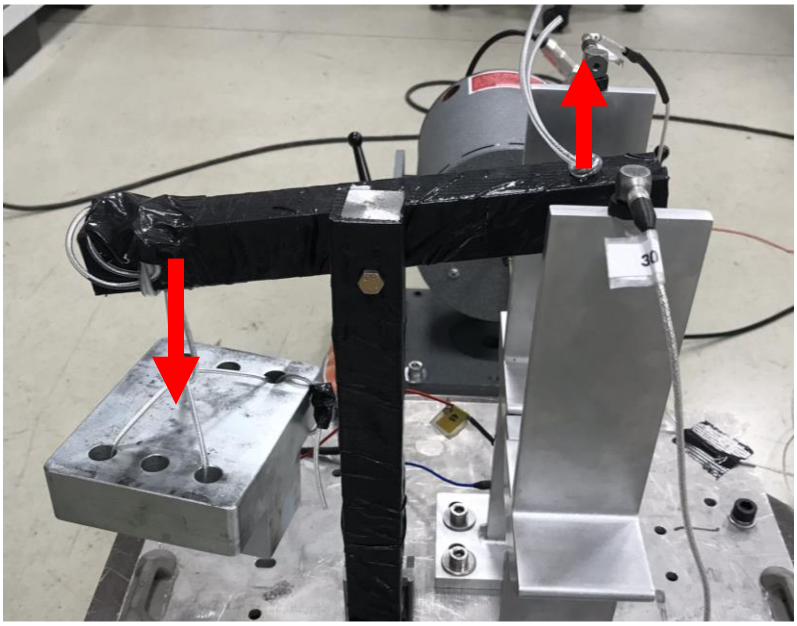

Figure 3.7. Leverage System for Normal Load Application

3.4. Excitation and Measurement System

The excitation and measurement system are same with the shrouded blade test setup. However, the accelerometers are replaced with 100g range for UPD test setup since there are no impact behavior. The complete test setup diagram together with excitation and measurement system is shown in Figure 3.8.

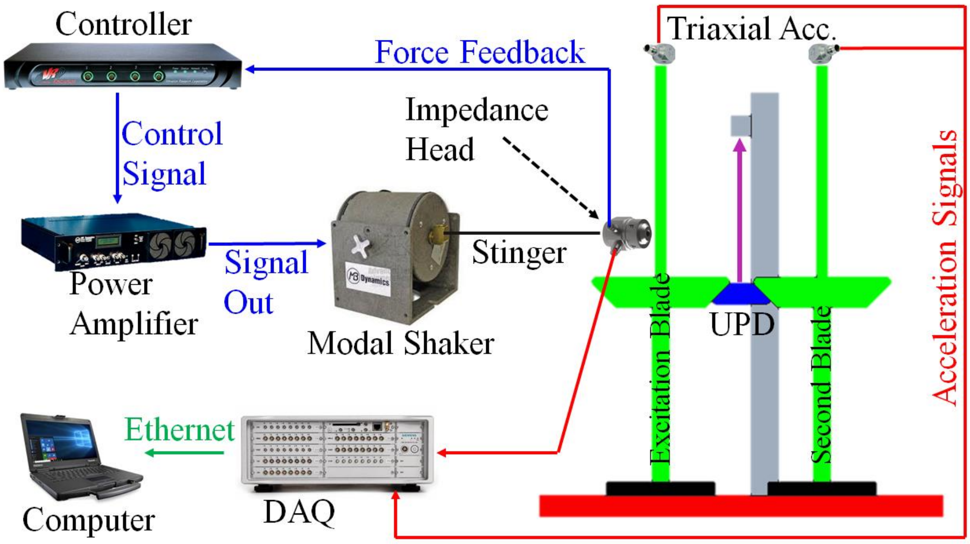

Figure 3.8. Excitation and Measurement System for Under Platform Damper Test Setup

The system is excited from 30 mm above the fixture surface which corresponds to 10% of the full height of the blade. Accelerometer responses are measured from the tip of the blades. First blade where the excitation is applied is named as excitation blade and the other one named as second blade for the naming purposes. Note that the accelerometer coordinates are mirrored in Y-Z plane. Therefore, correction is applied while comparing the phase between two blades which is shown in Figure 3.9.

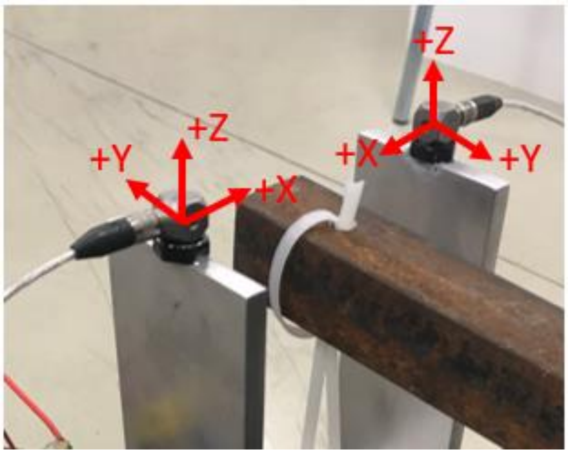

Figure 3.9. Cartesian Coordinate System of the UPD Test Setup

CHAPTER 4

TEST RESULTS

4.1. SHROUDED BLADE RESULTS

In order the observe the effect of different parameters on the dynamic response of the blades, controlled tests are conducted. Effect of different parameters which are shroud angle, the amount of initial gap, shroud position in radial direction and excitation amplitude are studied and the results are presented in this part. In order to excite the nonlinearity in the system sine sweep excitation is applied with a rate of 4 Hz/min. This rate is adjusted by pretests such that the nonlinear steady state response is obtained and the frequency range of interest is covered within a reasonable test duration.

In order to obtain the linear response of the shrouded blade system, gaussian white noise random vibration tests are conducted. By using random excitation, linear system natural frequencies are revealed quickly. Additionally, the linear system response is obtained by sine sweep excitation and it is observed that they match. Moreover, a linear harmonic analysis is performed in order to validate the test results.

Acceleration and displacement FRFs of the linear system at the blade tip is shown in Figure 4.1 for both random and sine sweep excitation in addition to analysis result. These results presented are for 10° shroud at the top position.

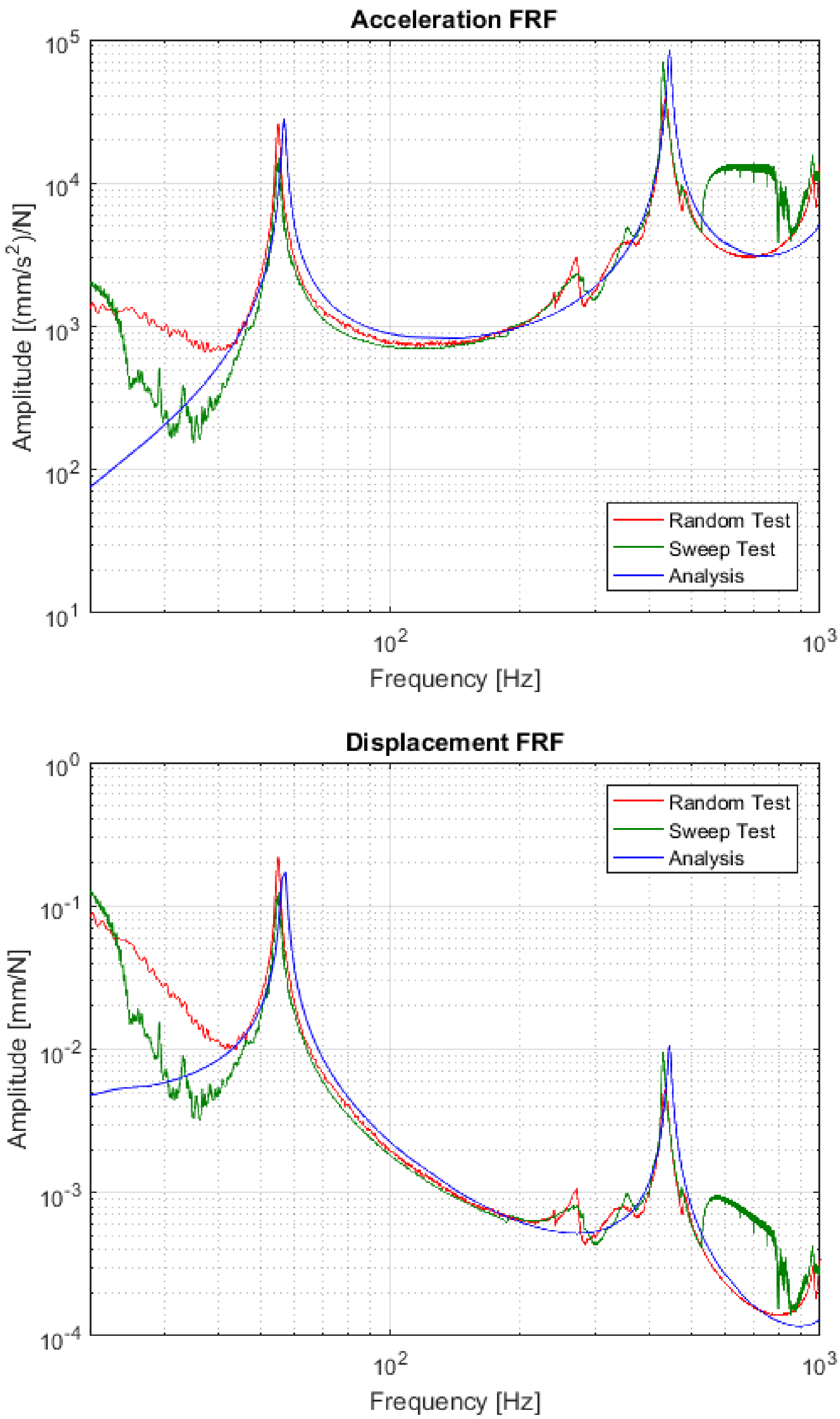

Figure 4.1. Linear System Acceleration and Displacement FRF of the Tip Point

From Figure 4.1, it can be seen that all three FRFs for both acceleration and displacement are consistent. There is a discrepancy between test and analysis results at low frequencies which is the nature of piezoelectrical sensors. These sensors measure the dynamic events and because of that DC shift occurs which amplifies more during integration. This effect can be reduced by applying a high-pass filter to the data. However, since these low frequencies are not in our frequency range of interest they are ignored.

Another difference between the test and analysis results is that there is a peak around 270 Hz at the test results. Referring *Table 2.1*, there is a lateral mode at 278 Hz and since in the real life it is not possible to excite the system exactly in one direction, we can see the lateral mode.

For the fixed free shrouded blade, 1st natural frequency of the system is obtained as 54.8 Hz from the tests whereas the analysis result is 57.4 Hz. The reason for this discrepancy is due to geometrical errors and the accelerometer mass at the tip point. Geometric tolerances of the blade dimensions, weld thickness at the blade root causing the boundary conditions differ from the simulation platform. In addition to these discrepancies, because of the accelerometer tip mass, there occurs difference between the analysis and test natural frequencies.

4.1.1. Effect of Excitation Amplitude

Firstly, the effect of excitation amplitude is studied. Initial gap is adjusted to 2 mm for all tests and the excitation amplitude is changed as 10, 20, 30, 40 and 60 N. The swept frequency range is adjusted to 30 – 70 Hz and the sweep rate is kept constant as 4 Hz/min. The effect of different excitation forces at the tip point displacement FRF are presented in Figure 4.2.

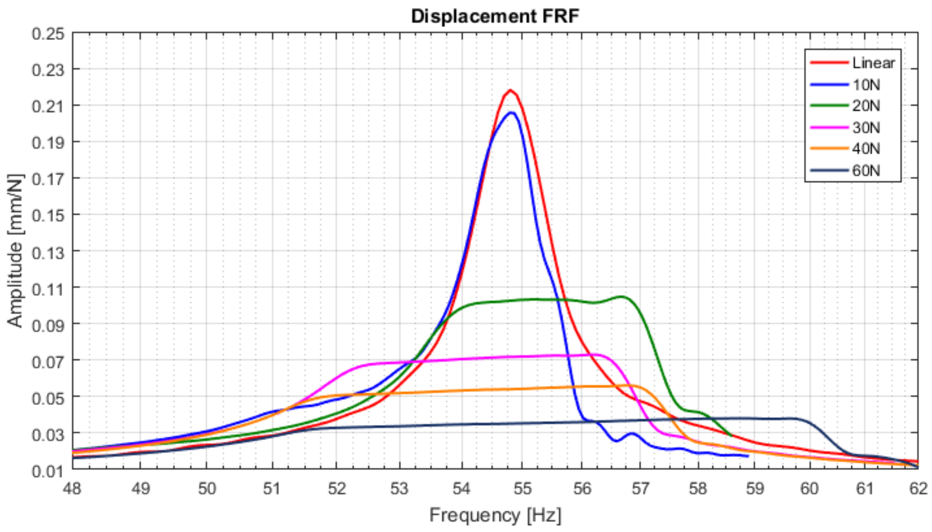

Figure 4.2. Displacement FRFs of Tip Point to Different Excitation Amplitudes

From Figure 4.2, it can be concluded that as the excitation amplitude increases the displacement response at the blade tip decreases since the shrouds contacts with the adjacent one for a longer time which results in more energy dissipation. Comparing linear and 10N excitation responses, one can conclude that the displacement amplitude does not change very much. This is due to the fact that tip point displacement is around 2.0mm when its excited by 10N excitation force for the linear system. Hence, when the excitation force is 10N there is a contact with the shroud for a very short time. Moreover, displacement amplitudes are obtained very close to 2.0mm when all the responses are multiplied by respective excitation forces.

4.1.2. Effect of Initial Gap

Secondly, the effect of initial gap is investigated. The initial gap between two contact surfaces is an important parameter for the design stage, because it has an effect on the contact status and the energy dissipation. Again, frequency range is adjusted to 30 - 70 Hz and sweep rate is kept constant as 4 Hz/min. The excitation force is adjusted to 40N and the initial gaps are changed as 2.0, 1.5, 1.2 and 1.0 mm. Resulting displacement FRF with 10° shroud is given in Figure 4.3 and 30° shroud results are presented in Figure 4.5. In both figures, "Linear" represents free response where there is no contact with the adjacent shrouds.

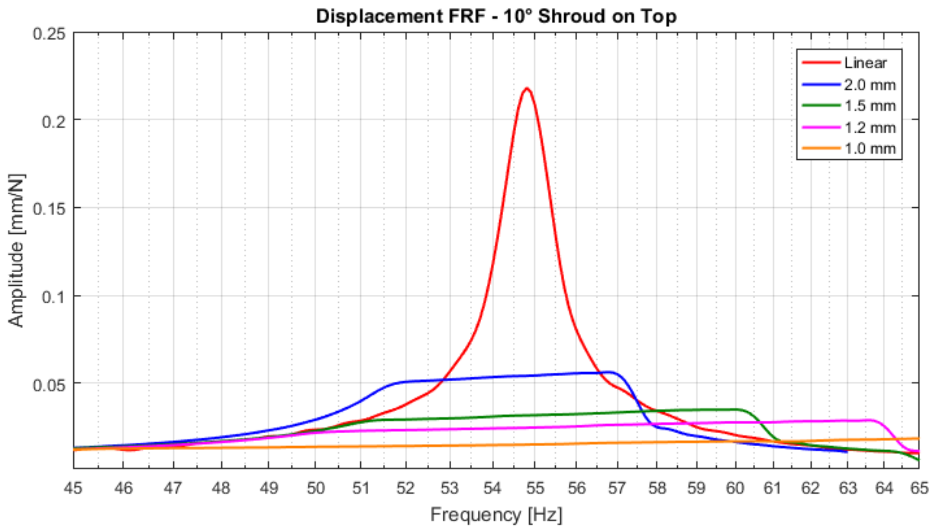

Figure 4.3. Displacement FRFs of Tip Point with 10° Shroud to Different Initial Gaps

Inspecting Figure 4.3, it can be clearly seen that the tip point displacement amplitude reduces greatly. As the initial gap between the shrouds decreases, the peak amplitude decreases and contact frequency range increases. Additionally, time domain responses of the blade tip point for the 10° shroud and 30° shroud are shown in Figure 4.4 and Figure 4.6, respectively. It can be seen that the intended and real gap amounts differ a little which is due to the adjustment error of the initial gap before the test.

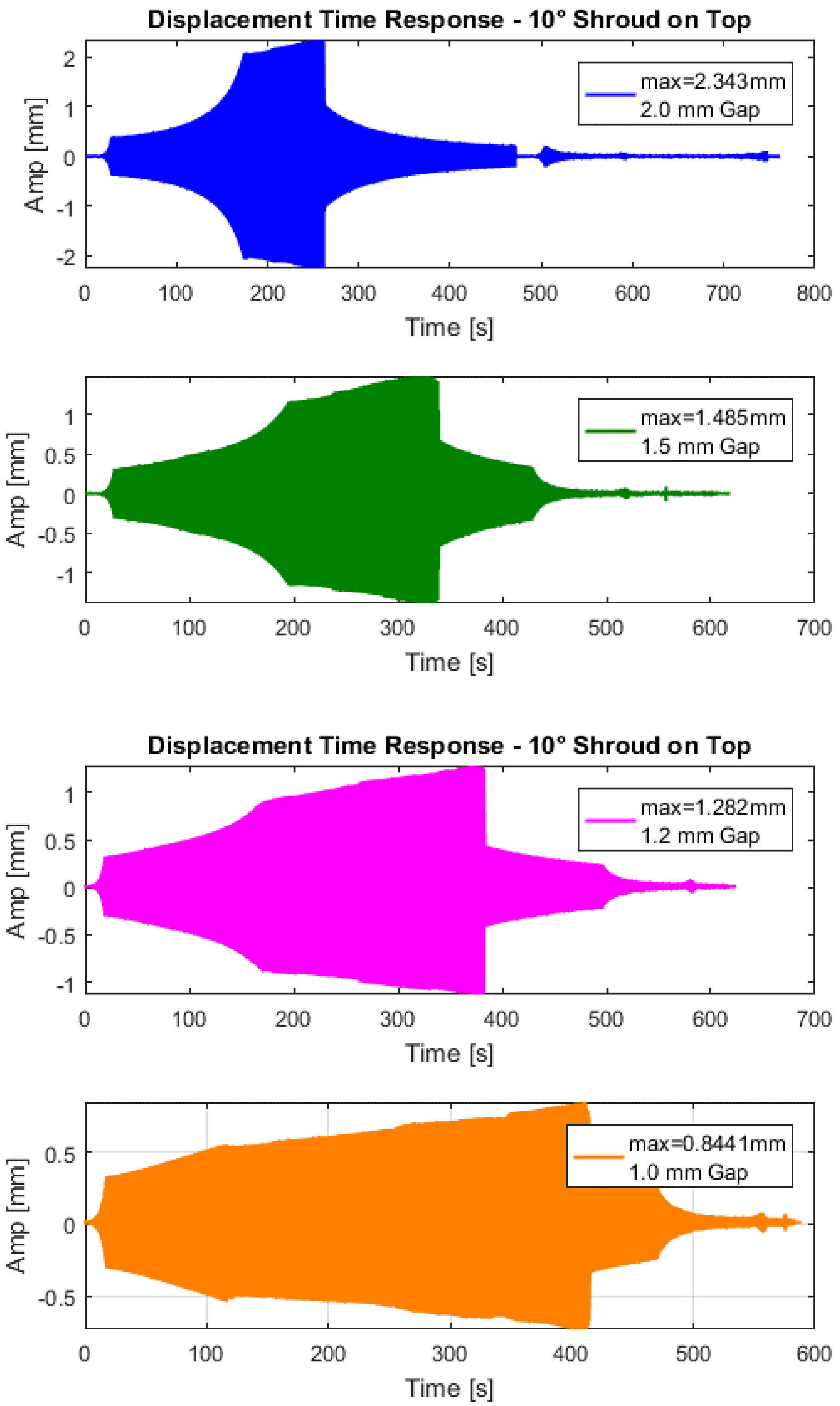

Figure 4.4. Tip Point Time Domain Displacements of 10° Shroud with Different Initial Gaps

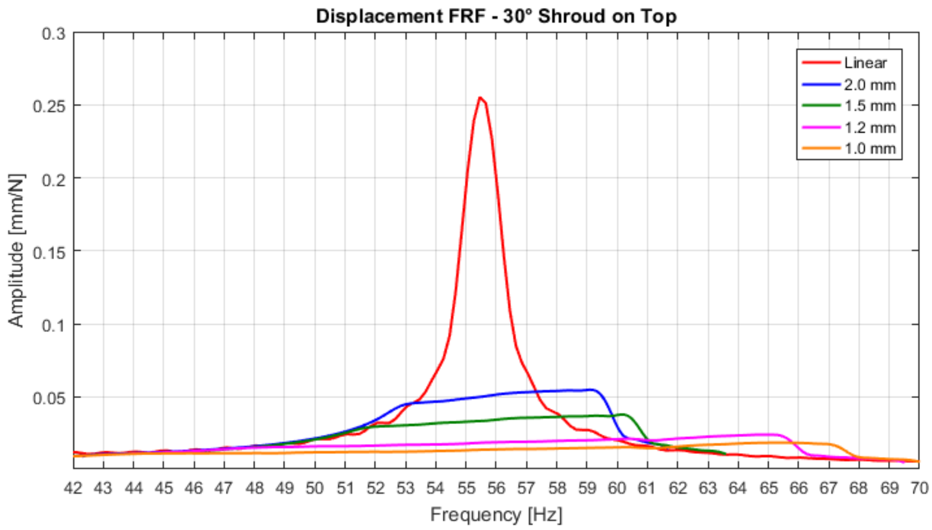

Figure 4.5. Displacement FRFs of Tip Point with 30° Shroud to Different Initial Gaps

Inspecting the results given in Figure 4.3 and Figure 4.5 it is clearly seen that as the initial gap between the shrouds decreases, the effect of friction damping increases and as a result the peak amplitude decreases. Moreover, since there are 10° and 30° shroud angle, the effect of friction is present in the nonlinear responses. This comparison is explained in detail in the following section. Additionally, by inspecting the time domain displacement responses the amount of initial gap limits the system go further and decreases the amplitude.

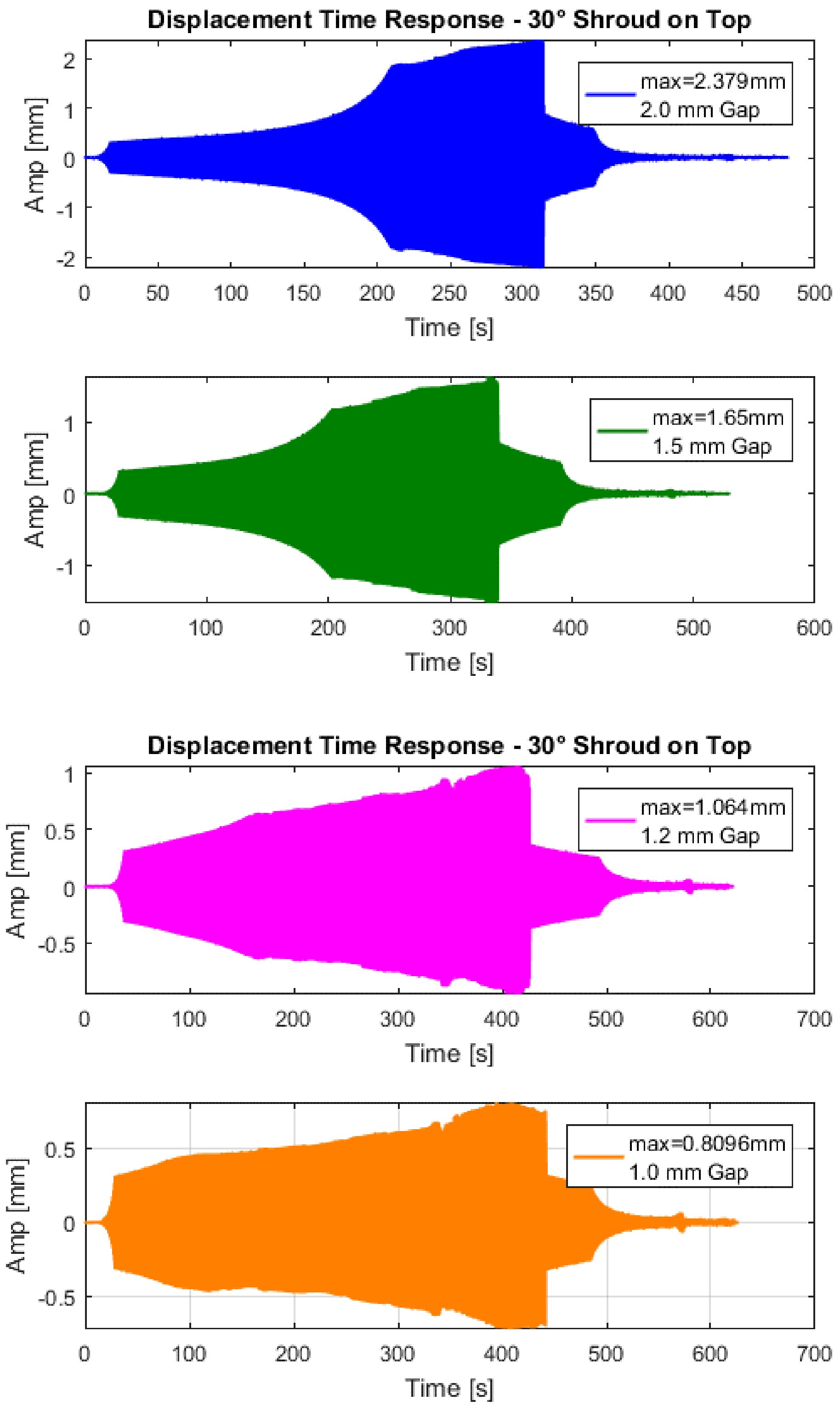

Figure 4.6. Tip Point Time Domain Displacements of 30° Shroud with Different Initial Gaps

4.1.3. Effect of Shroud Angle

Thirdly, the effect of different shroud angles is studied. Two different shroud angles which are 10° and 30° are used during the tests and the tip point displacement FRF graphs are compared. Initial gap amounts are again adjusted to 2.0, 1.5, 1.2 and 1.0 mm for both shroud angle. Resulting graphs are shown in Figure 4.7, Figure 4.8, Figure 4.9 and Figure 4.10, respectively.

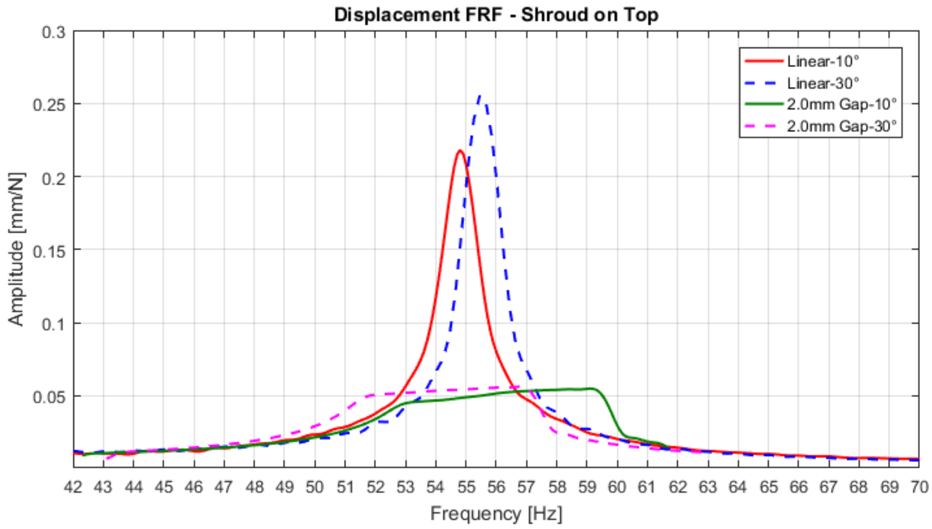

Figure 4.7. Displacement FRFs of Tip Point with 10° and 30° shroud with initial gap of 2.0mm

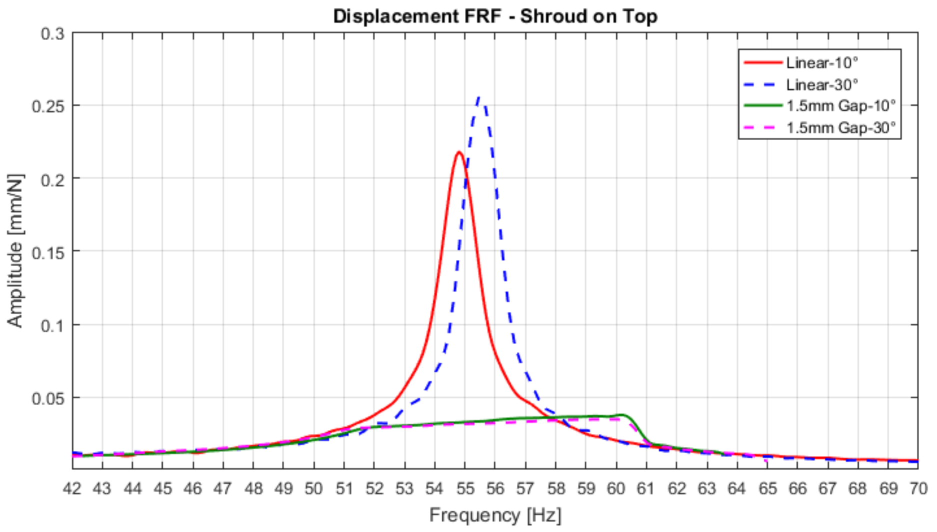

Figure 4.8. Displacement FRFs of Tip Point with 10° and 30° shroud with initial gap of 1.5mm

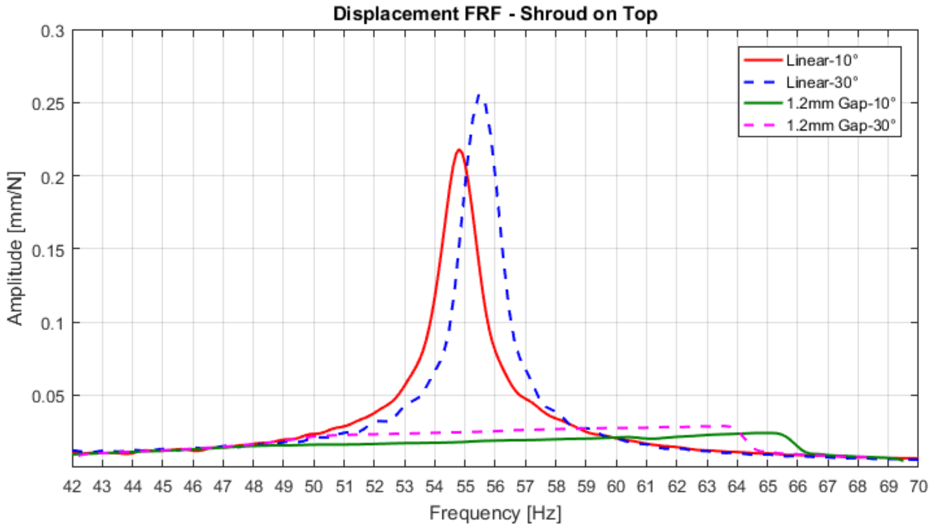

Figure 4.9. Displacement FRFs of Tip Point with 10° and 30° shroud with initial gap of 1.2mm

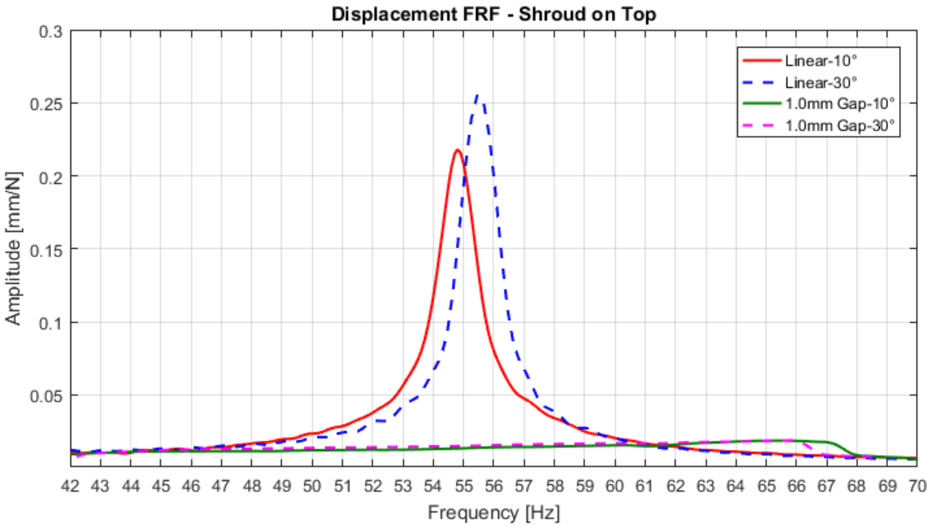

Figure 4.10. Displacement FRFs of Tip Point with 10° and 30° shroud with initial gap of 1.0mm

Mass of the 10° and 30° shrouds are 134 and 127 grams, respectively. Since there are two shrouds at the tip point of the blade, the mass difference is 14 grams in total. When the linear responses are compared this difference can be observed. Natural frequency of the 10° system is approximately 1 Hz lower than the 30° shroud system which are 54.8 Hz and 55.5 Hz, respectively.

4.1.4. Effect of Shroud Position

The effect of shroud position along radial direction is also investigated. There are three possible mounting position which are top, middle and bottom. Top corresponds to the tip point of the blade; middle mounting position is 40mm below the blade tip and at the bottom configuration shrouds are placed 80mm below the blade tip. Alternatively, in order to eliminate the dependency on the blade length; top, middle and bottom positions are referred as 100%, 90% and 80% length of the blade respectively.

Firstly, shrouds are placed on top position and the resulting displacement FRF graph is shown at Figure 4.11. with 2.0, 1.5, 1.2 and 1.0mm initial gaps.

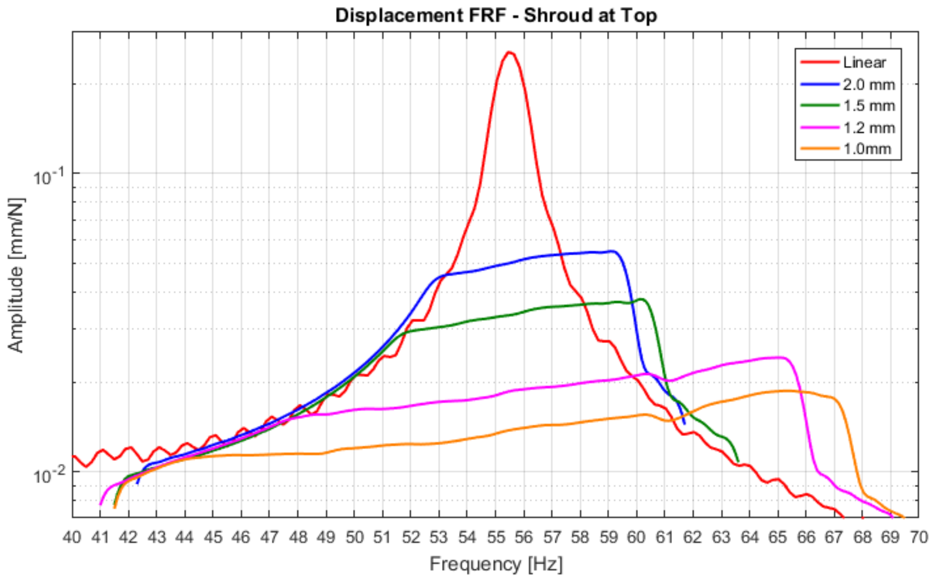

Figure 4.11. Displacement FRFs of Tip Point with Shroud on Top

From Figure 4.11, it can be seen that the peak tip point displacement amplitude reduces from 0.25mm to 0.05mm for 2.0mm initial gap case.

Afterwards, the shroud is mounted on middle position which is 90% of the total length. The resulting tip point displacement FRFs are presented in Figure 4.12 with 2.0mm, 1.8mm and 1.5mm initial gap.

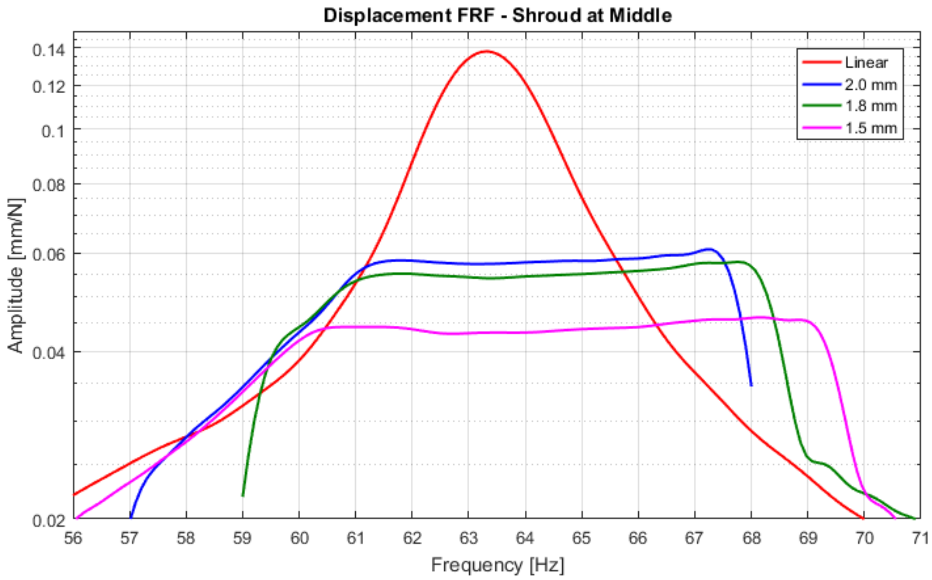

Figure 4.12. Displacement FRFs of Tip Point with Shroud at Middle

From Figure 4.12, for the 2.0 mm initial gap, the peak response amplitude reduces down to 0.06mm from 0.14mm. Note that the gap amount is adjusted at the shroud contact position along the radial direction, however responses are measured from the tip point.

Finally, shroud is mounted on bottom position which corresponds to 80% of the total length. The resulting tip point displacement FRFs are presented in Figure 4.13 with 2.0 and 1.5mm initial gap.

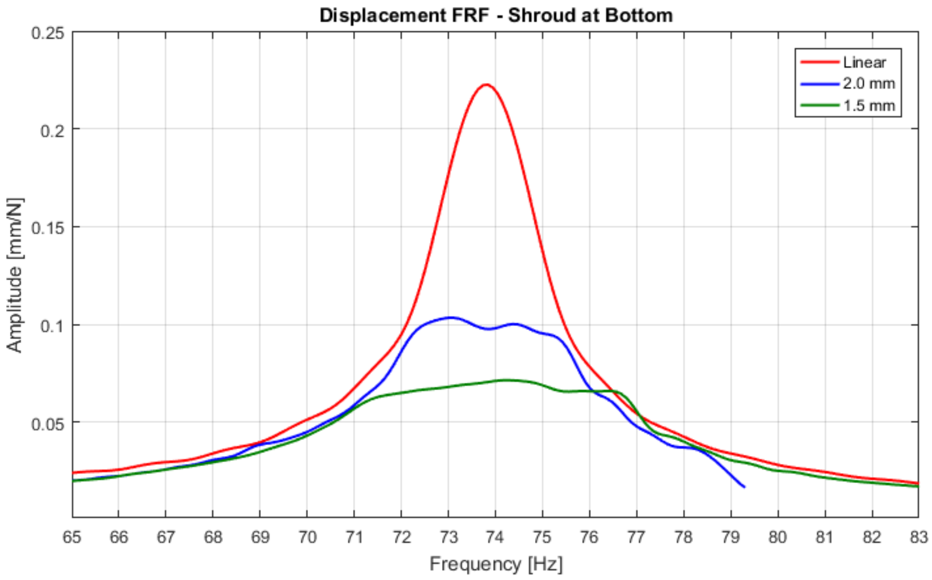

Figure 4.13. Displacement FRFs of Tip Point with Shroud at Bottom

From Figure 4.13, for the 2.0 mm initial gap, the peak response amplitude reduces down to 0.10mm from 0.22mm. Note that the gap amount is adjusted at the shroud contact position along the radial direction, however responses are measured from the tip point.

Comparison between these three shroud positions on peak amplitude reduction is tabulated in *Table 4.1* for different initial gap scenario. Reduction ratios are obtained by scaling the nonlinear peak response amplitudes to the linear peak amplitude response.

Table 4.1. *Effect of Shroud Position on Radial Direction*

Peak Amplitude Reduction Ratio			
Amount of Initial Gap [mm]	**Shroud Position**		
	Top	**Middle**	**Bottom**
2.0	80.4%	58.4%	56.1%
1.5	86.9%	68.7%	68.3%
1.0	94.6%	N/A	N/A

From *Table 4.1*, it can be seen that as the amount of initial gap decreases the amplitude reduction increases. Another outcome is that there is an optimum point for which the amplitudes are minimum. It can be seen from the results that the reduction ratio decreases when the shroud is shifted down from top position to the middle position. However, further shifting down the shroud to the bottom does not decrease the reduction ratio as the first case. For the above experimental setup top position is the best position for the amplitude reduction among three positions.

4.2. UNDER PLATFORM DAMPER RESULTS

Designed under platform damper test setup is first analyzed by including the under platform damper contact in the model. The contact surfaces are connected by defining normal and tangential stiffnesses at the interface. Then, by changing the stiffness values effect of the changing normal loads are simulated. In phase and out of phase modes are determined for different contact stiffnesses. After that the tests are conducted and compared with the simulation results.

During the analysis 10 different contact stiffness combinations are produced and the resulting IP and OoP modes are tabulated in *Table 4.2*.

Table 4.2. *Simulation Scenario & IP – OoP Modes*

UPD Simulation Results				
Scenario	**Normal Stiffness**	**Tangential Stiffness**	**In-Phase Mode**	**Out-of-Phase Mode**
	[N/mm]	**[N/mm]**	**[Hz]**	**[Hz]**
1	$1x10^2$	$5x10^2$	110.2	206.7
2	$5x10^2$	$5x10^2$	121.9	213.4
3	$1x10^3$	$1x10^3$	133.3	219.6
4	$1x10^4$	$1x10^4$	196.7	243.7
5	$5x10^4$	$1x10^4$	208.3	246.7
6	$5x10^4$	$5x10^4$	210.6	247.2
7	$5x10^4$	$1x10^5$	224.4	250.1
8	$5x10^4$	$1x10^6$	226.2	250.5
9	$5x10^4$	$1x10^9$	226.4	250.5
10	$1x10^9$	$1x10^9$	230.7	251.3

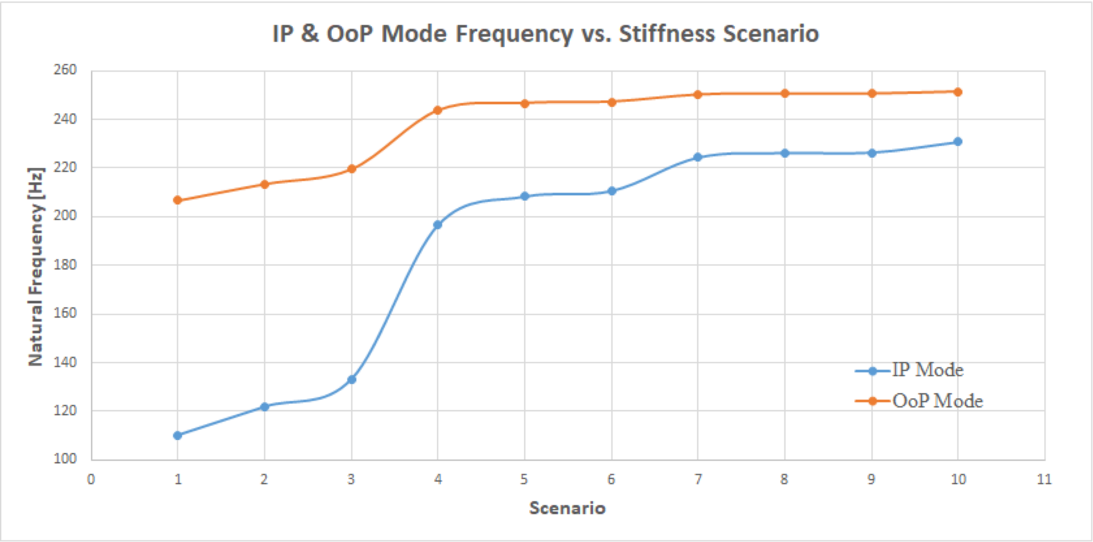

Figure 4.14. Effect of Contact Stiffness on IP and OoP Mode Frequency

From Figure 4.14, the effect of changing contact stiffness on IP and OoP modes can be analyzed. As the contact stiffness between the UPD and the blades decreases, IP and OoP natural frequencies decreases. However, IP mode is affected by the stiffness more than OoP mode. Moreover, there is a region between scenario 3 and scenario 4 where the contact stiffness sensitivity increases. However, this study is conducted in order to observe the effect of normal load at the contact interface and does not represent the nonlinear simulation. In the real nonlinear contact, normal load at the contact interface changes depending on the contact state. As the normal load at the interface decreases there will occur separation other than stick and slip states. Also, in the simulations the defined contact stiffnesses will have a pulling effect whereas in the real case the normal load plays role only in the normal load application direction. Therefore, analysis results can be used to determine only fully stuck scenario with a very high contact stiffness value.

Modal analysis results for all contact stiffness scenario are presented in from Figure 4.15 to Figure 4.24.

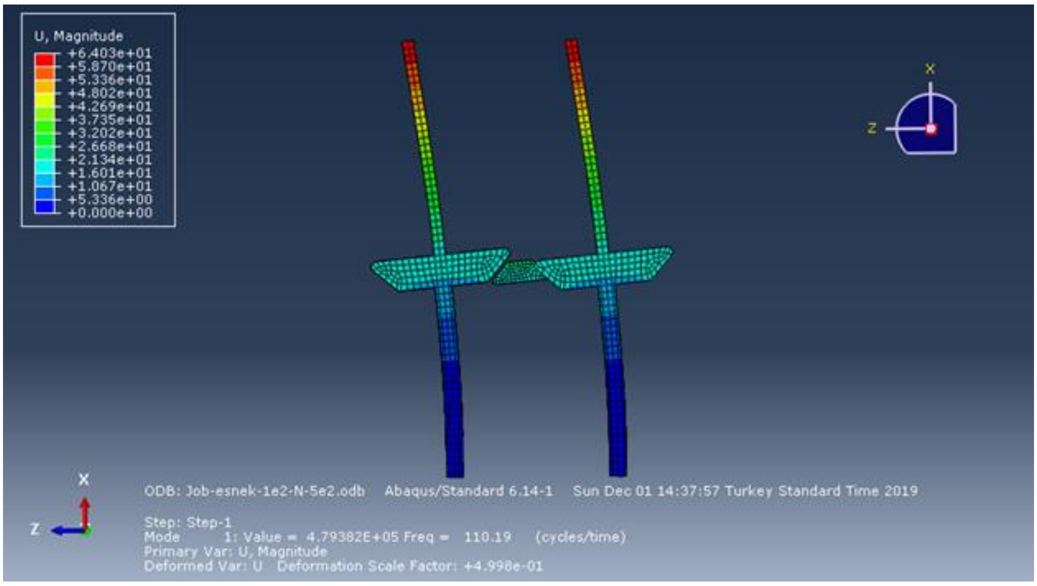

In Phase (IP) Mode

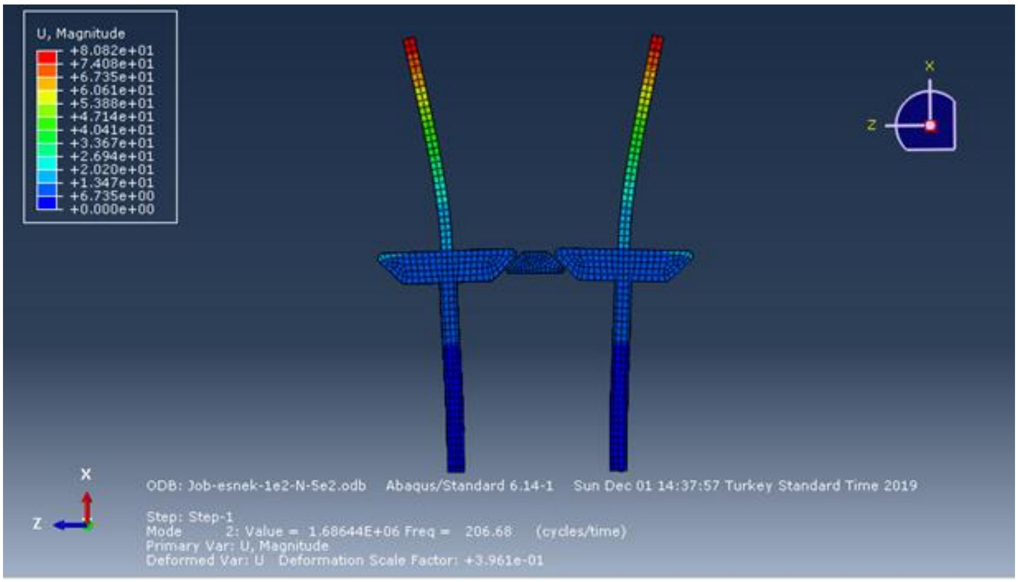

Out of Phase (OoP) Mode

Figure 4.15 In Phase and Out of Phase Modes – Scenario 1

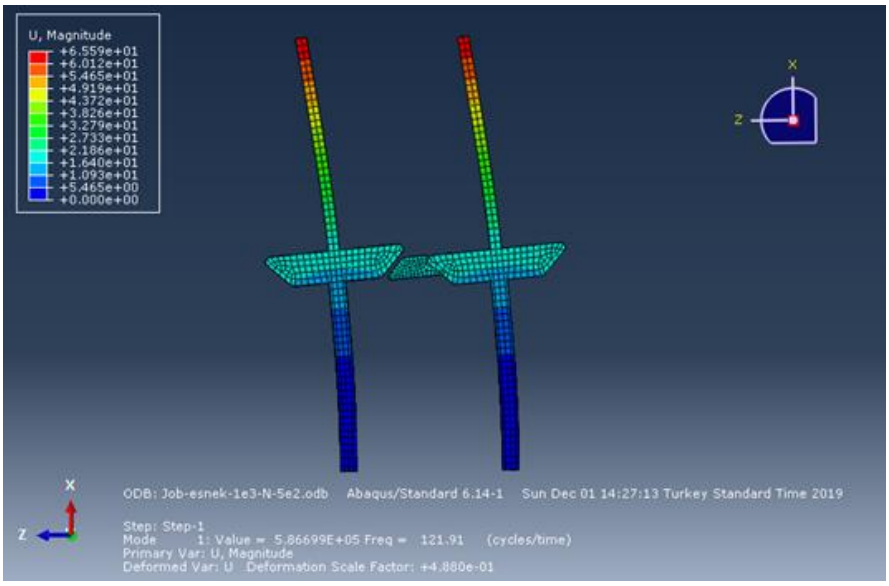

In Phase (IP) Mode

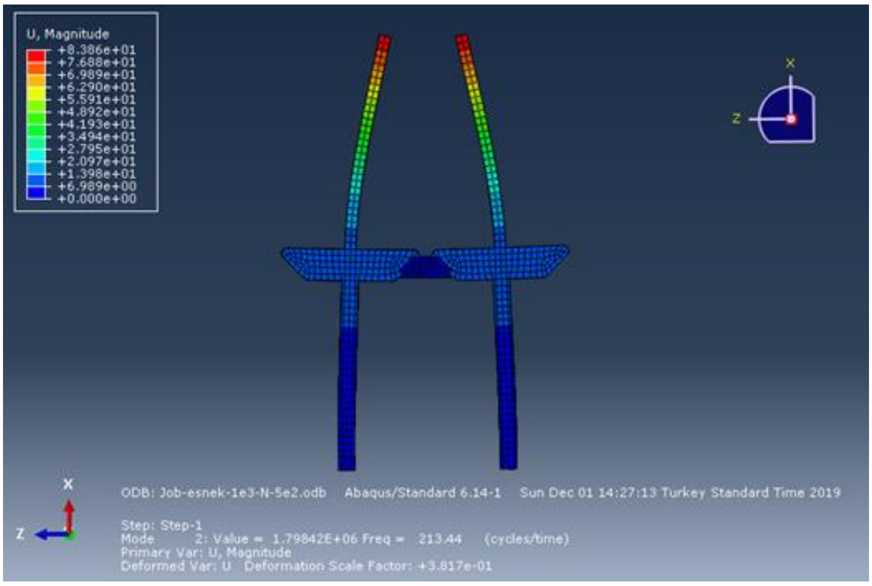

Out of Phase (OoP) Mode

Figure 4.16 In Phase and Out of Phase Modes – Scenario 2

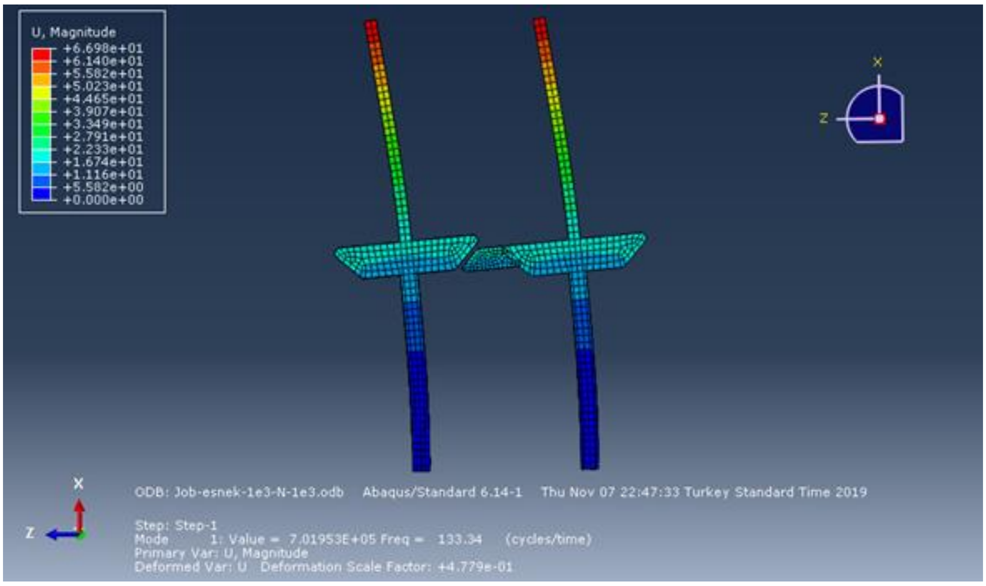

In Phase (IP) Mode

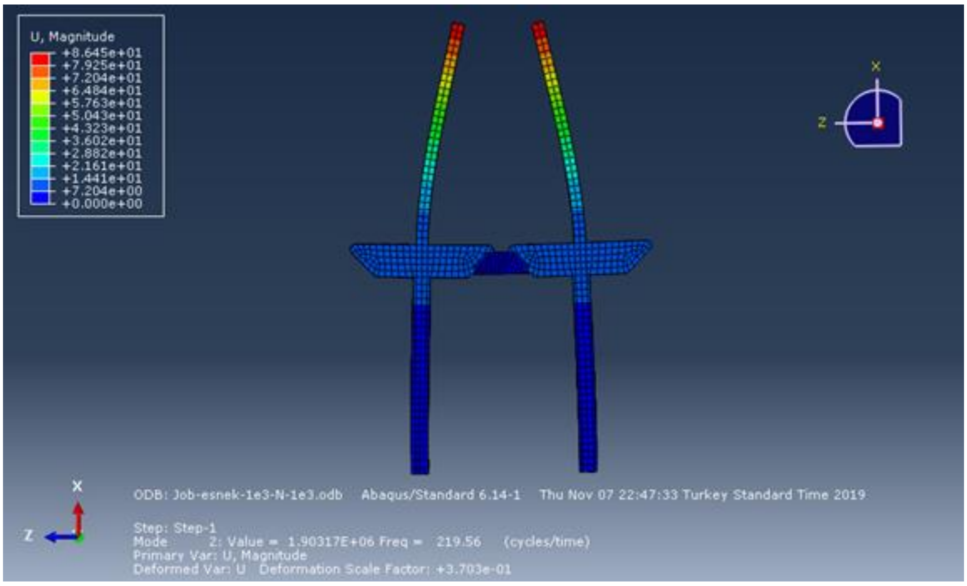

Out of Phase (OoP) Mode

Figure 4.17 In Phase and Out of Phase Modes – Scenario 3

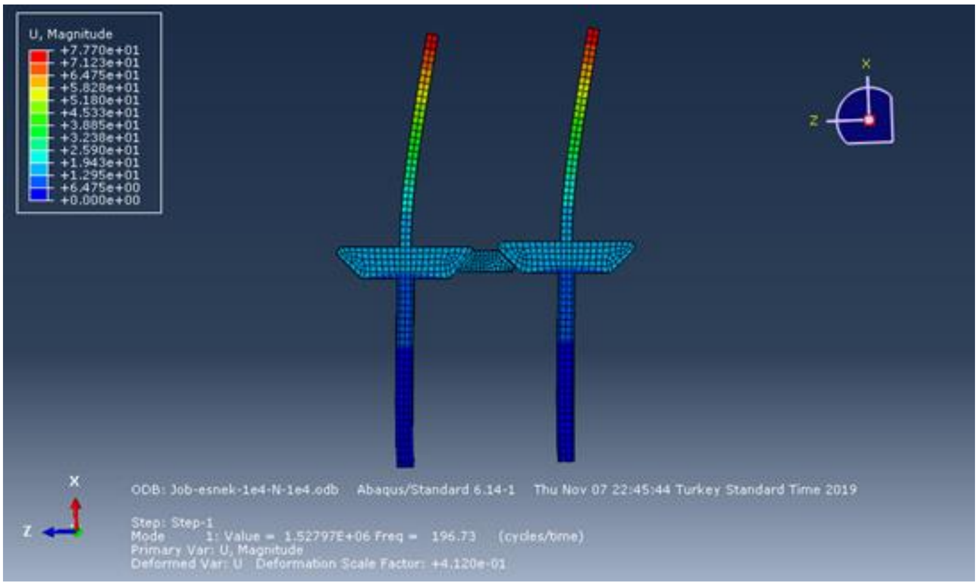

In Phase (IP) Mode

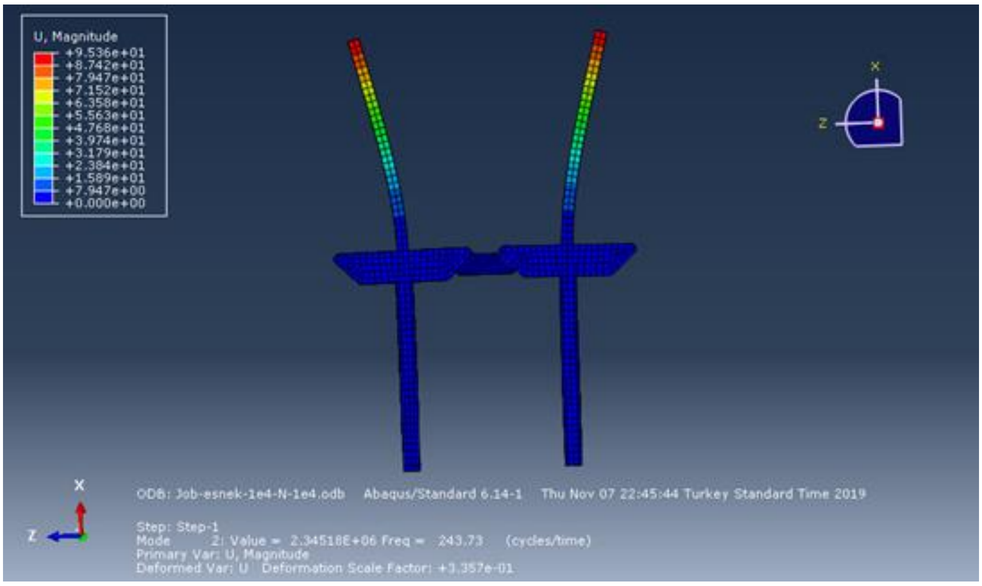

Out of Phase (OoP) Mode

Figure 4.18 In Phase and Out of Phase Modes – Scenario 4

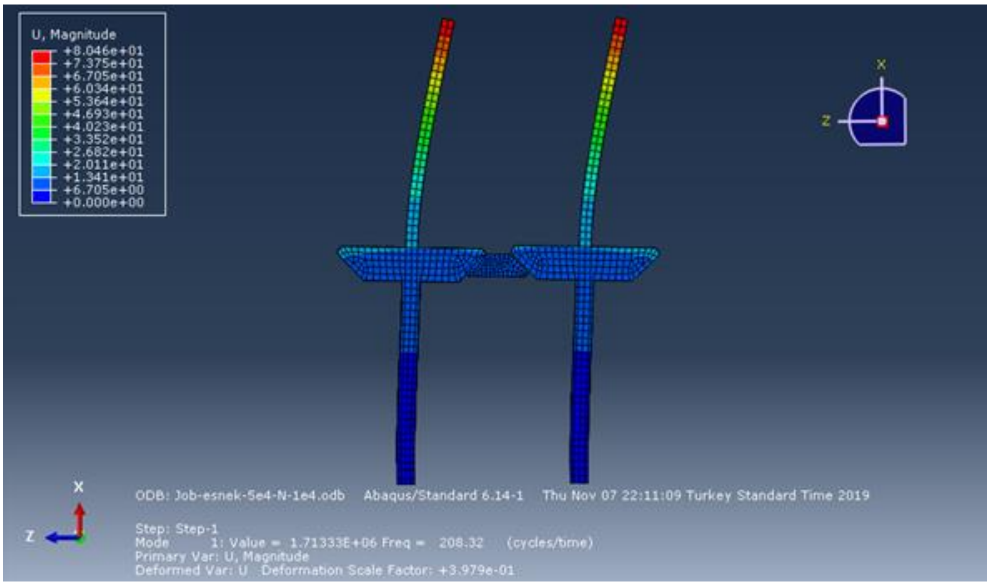

In Phase (IP) Mode

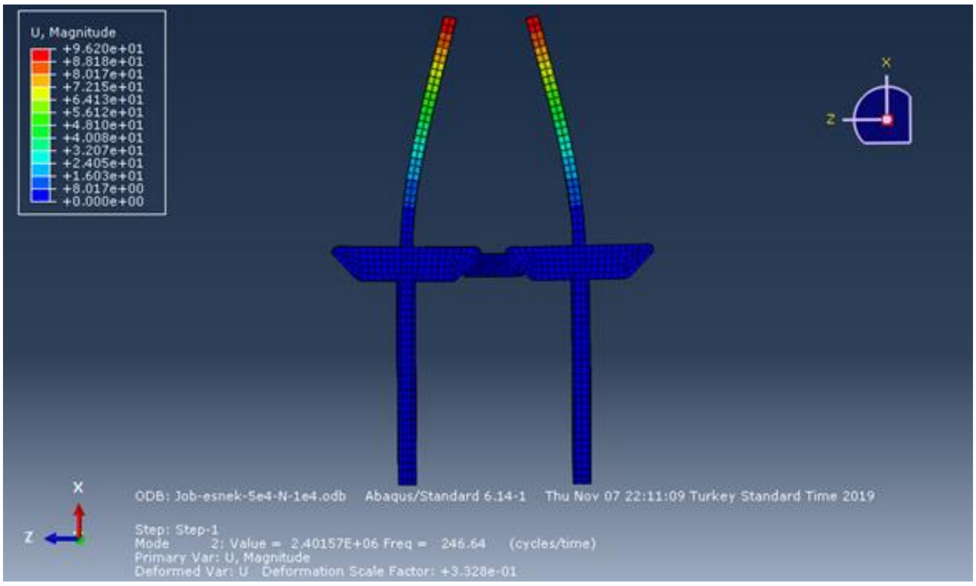

Out of Phase (OoP) Mode

Figure 4.19 In Phase and Out of Phase Modes – Scenario 5

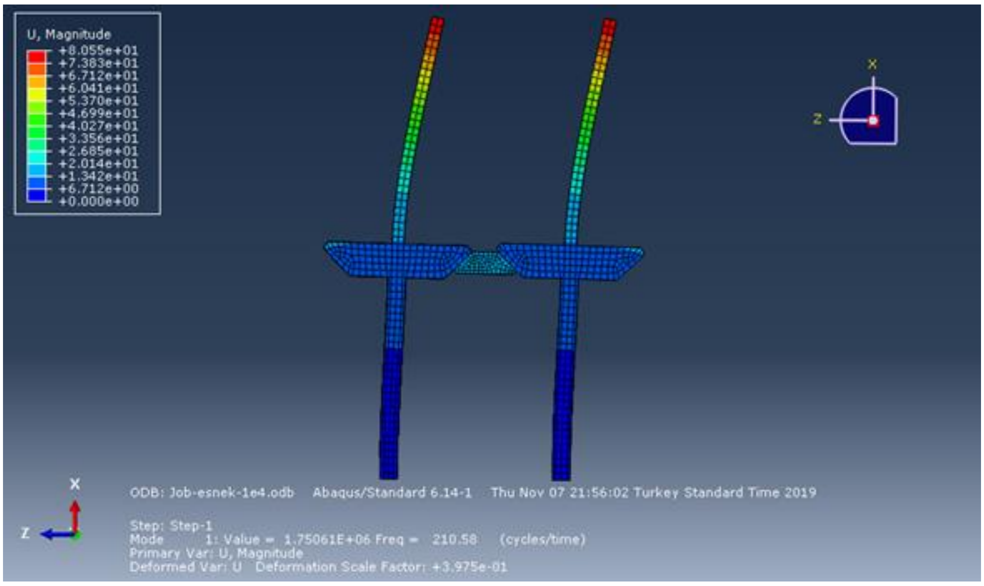

In Phase (IP) Mode

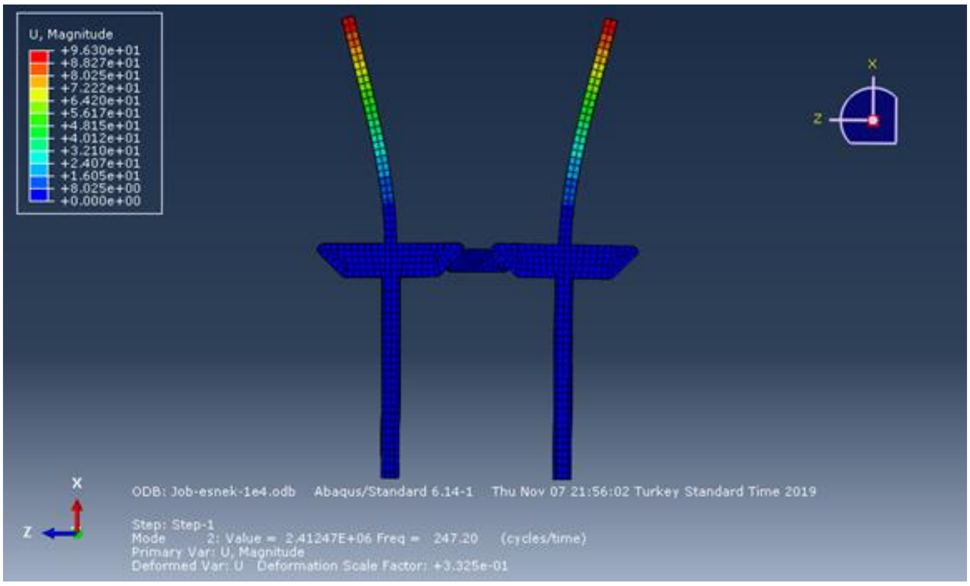

Out of Phase (OoP) Mode

Figure 4.20 In Phase and Out of Phase Modes – Scenario 6

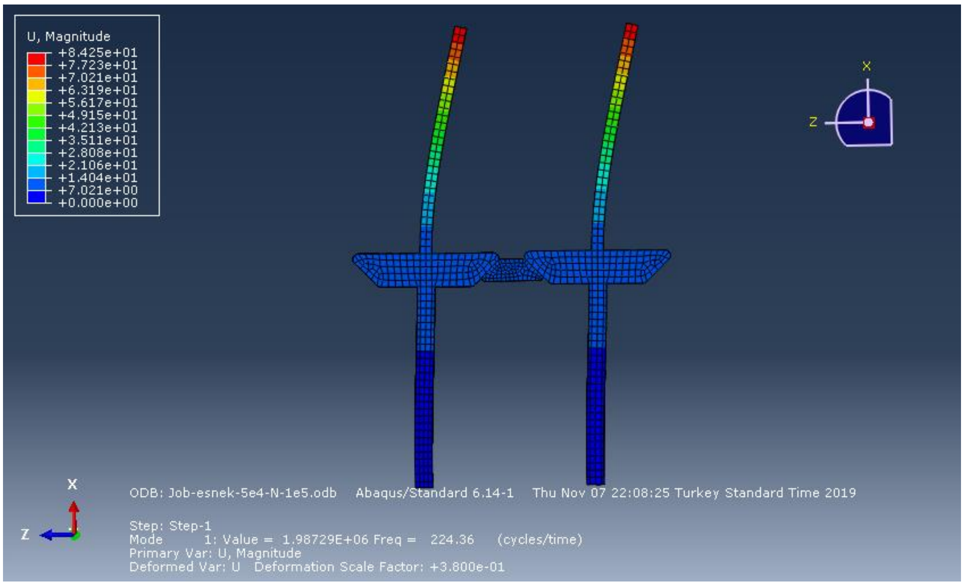

In Phase (IP) Mode

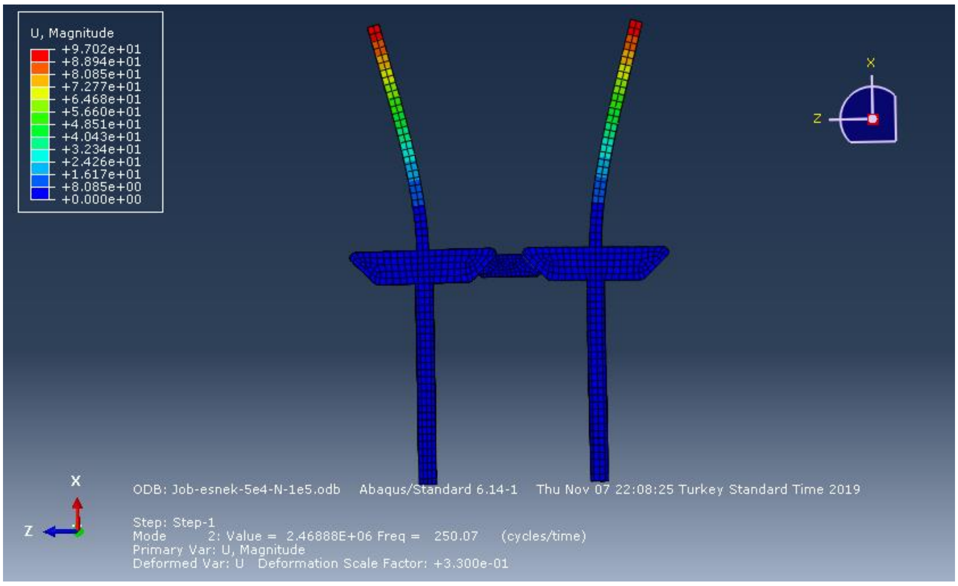

Out of Phase (OoP) Mode

Figure 4.21 In Phase and Out of Phase Modes – Scenario 7

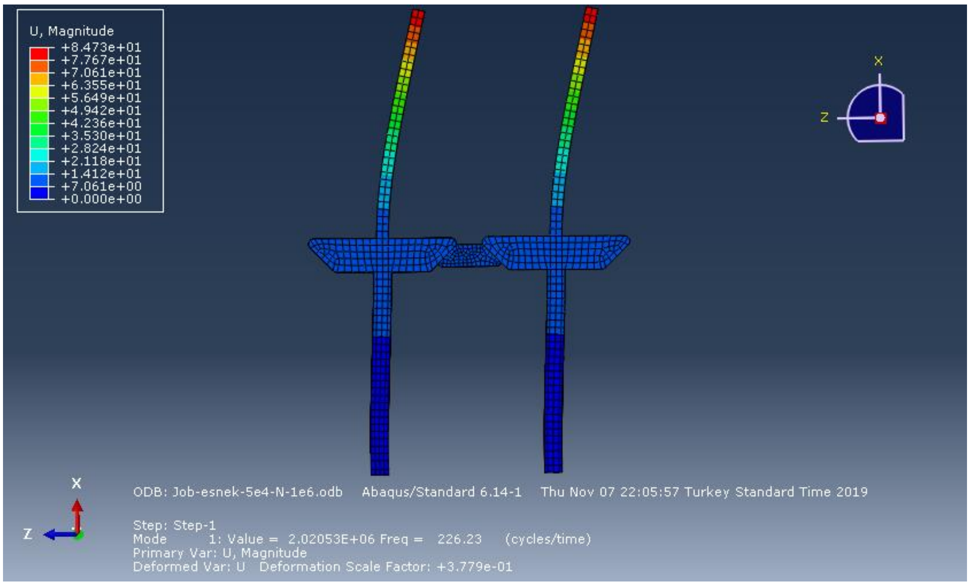

In Phase (IP) Mode

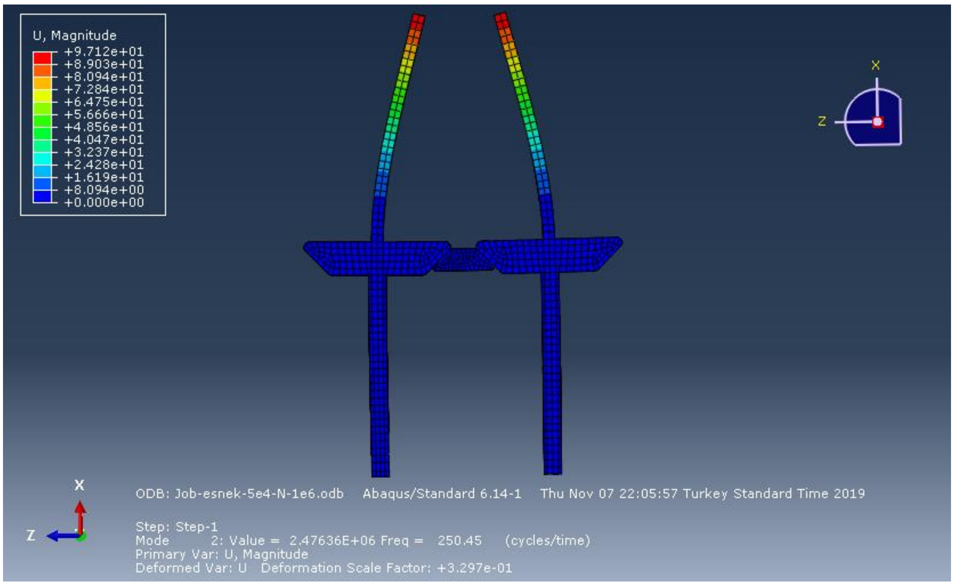

Out of Phase (OoP) Mode

Figure 4.22 In Phase and Out of Phase Modes – Scenario 8

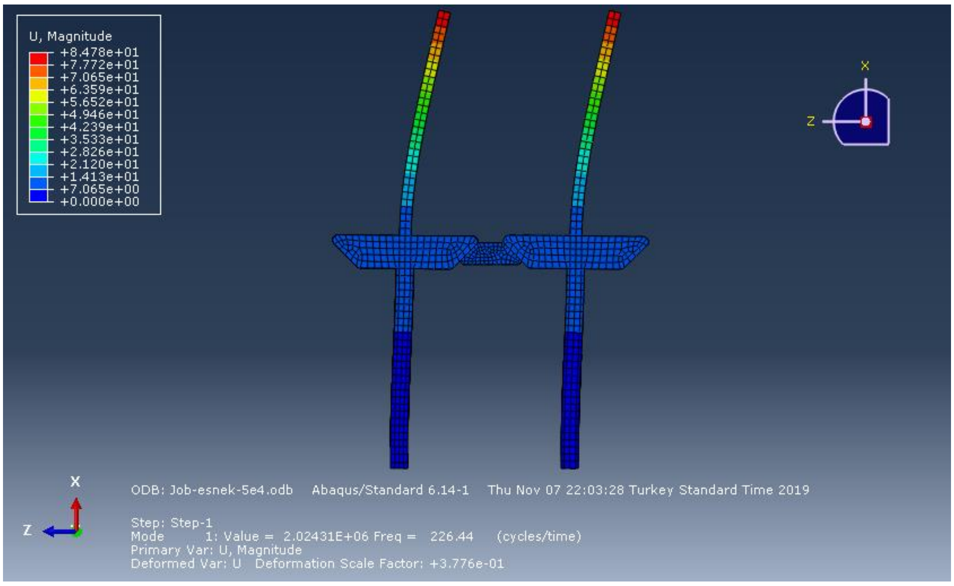

In Phase (IP) Mode

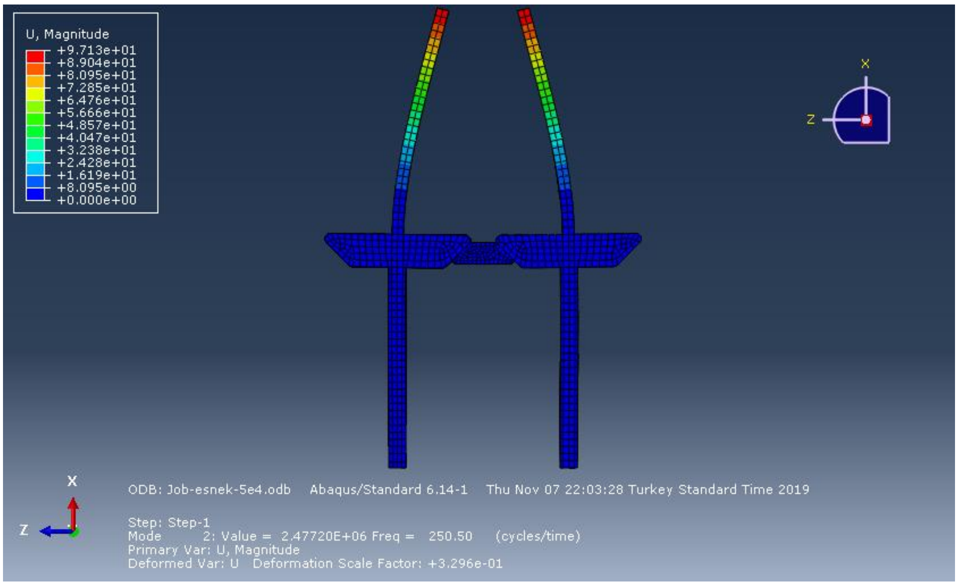

Out of Phase (OoP) Mode

Figure 4.23 In Phase and Out of Phase Modes – Scenario 9

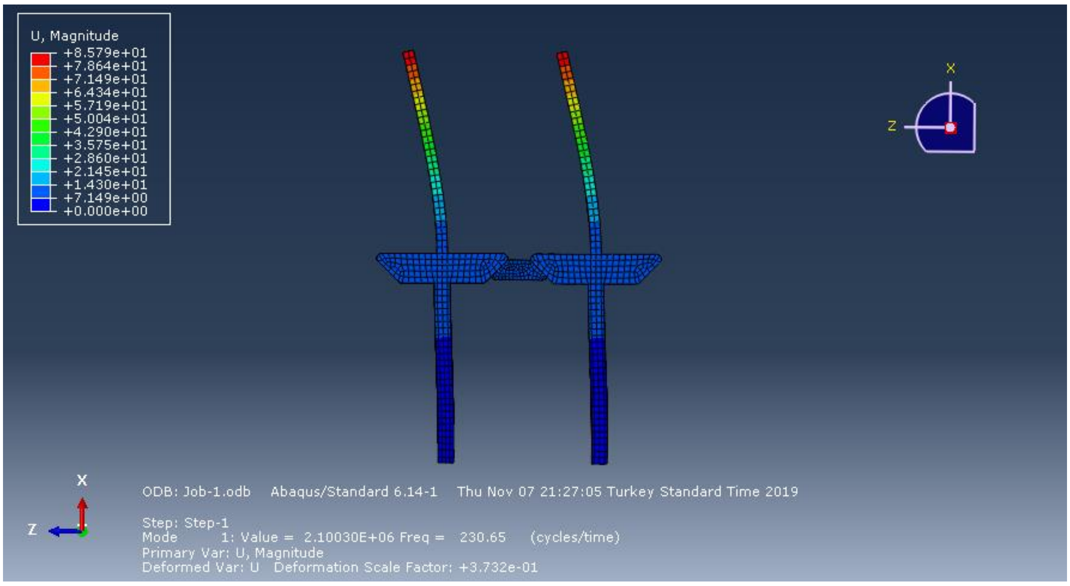

In Phase (IP) Mode

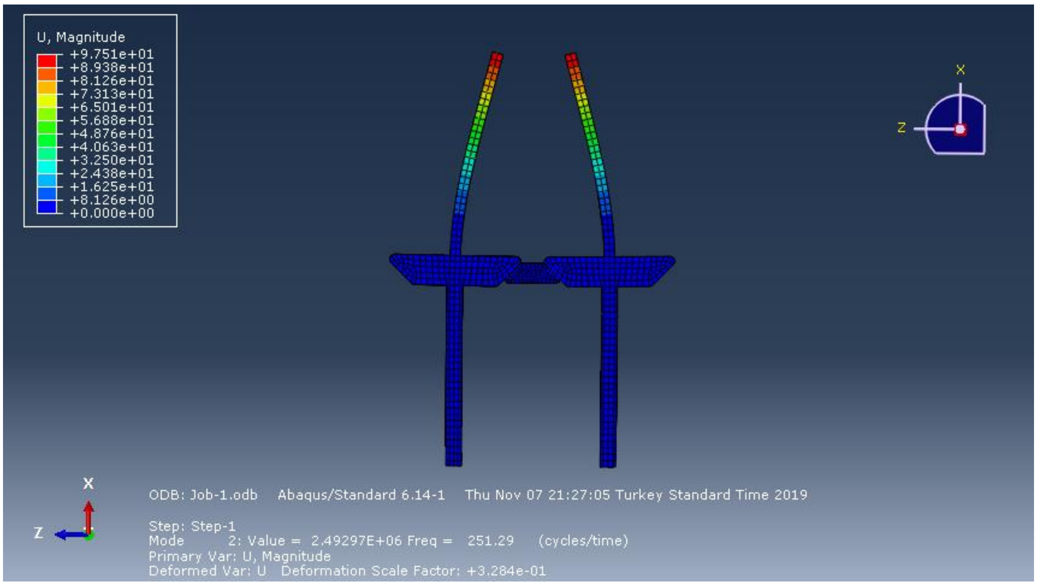

Out of Phase (OoP) Mode

Figure 4.24 In Phase and Out of Phase Modes – Scenario 10

After the analyses, the test conditions are determined and several tests are conducted with UPD test setup. The system is excited from 30mm above the base plate and the responses are measured from the tip point of the blades. The effect of different excitation amplitude is studied.

Firstly, the linear response of the blade is obtained by applying gaussian white noise random vibration. A wide frequency range can be excited with random excitation and the resulting linear response is presented in Figure 4.25.

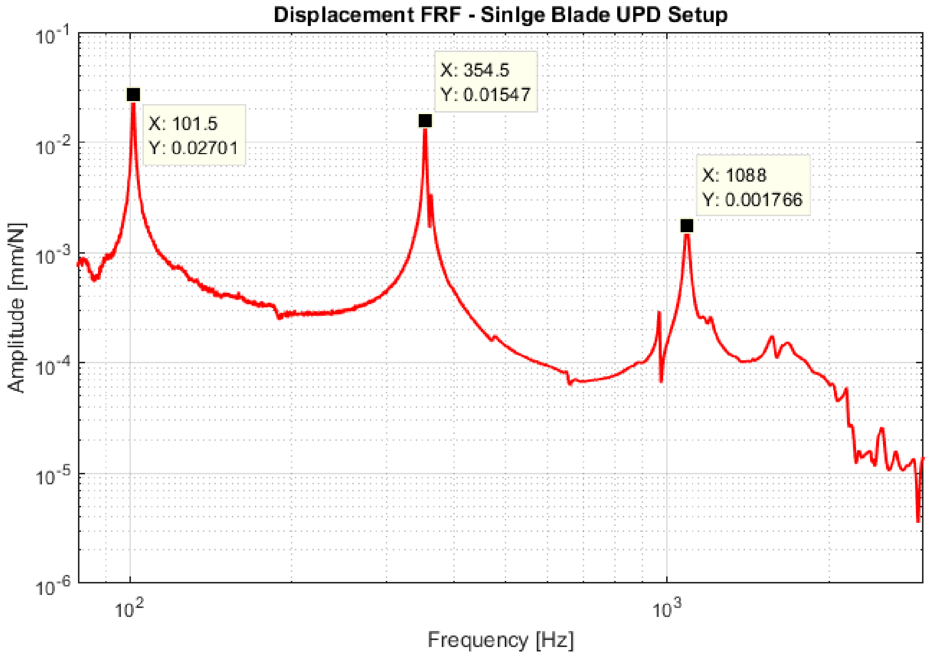

Figure 4.25. Linear Displacement FRF of the Tip Point in X Direction

Comparing test results presented in Figure 4.25 the modal analysis results which are given in Figure 3.3 it can be seen that they agree. The first mode was calculated as 100.5 Hz and it is measured as 101.5 Hz. Also, second bending mode was calculated as 352.2 Hz and measured as 354.5 Hz. Note that there are some small differences and these result from the geometric tolerances, material density etc. Moreover, the lateral bending and torsional responses are not revealed which are calculated at 505.9 Hz and 633.3 Hz. This situation implies that the excitation is applied in X direction quite well for the experimental case.

4.2.1. Effect of Excitation Amplitude

For the nonlinear analyses, firstly the effect of excitation amplitude is investigated. Six different excitation amplitudes are selected which are 0.1 N, 1N, 20N, 40N, 80N and 160 N. The normal load applied at the contact interface is kept constant as 44N. Accelerometer responses are measured from the tip point of both blades and IP and OoP modes are obtained. Additionally, UPD is fixed to the contact interface with glue in order to represent the very high normal force at the contact interface.

For the frequency range of 40-400 Hz with a sweep rate of 10 Hz/min, the resulting displacement FRFs and phase angle are shown below for both excitation and second blades in excitation direction.

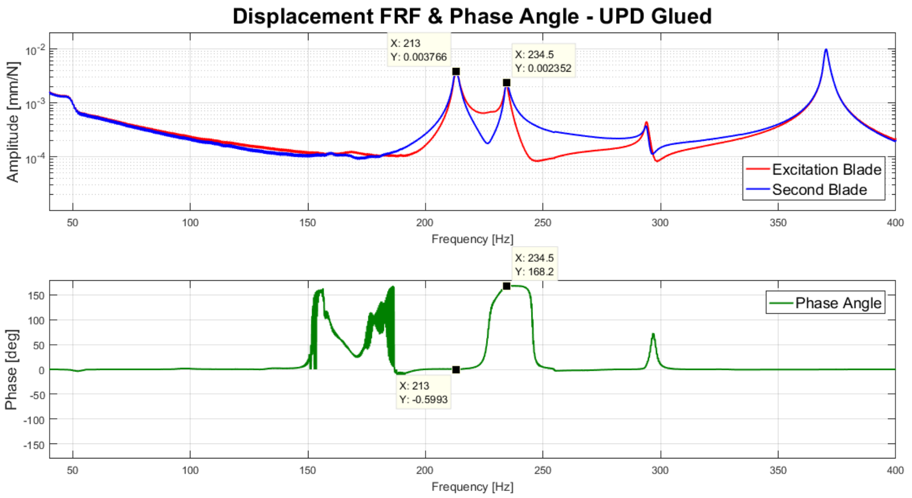

Figure 4.26. Displacement FRFs and Phase Angle of Tip Points of Both Blades in X Direction for Fixed UPD

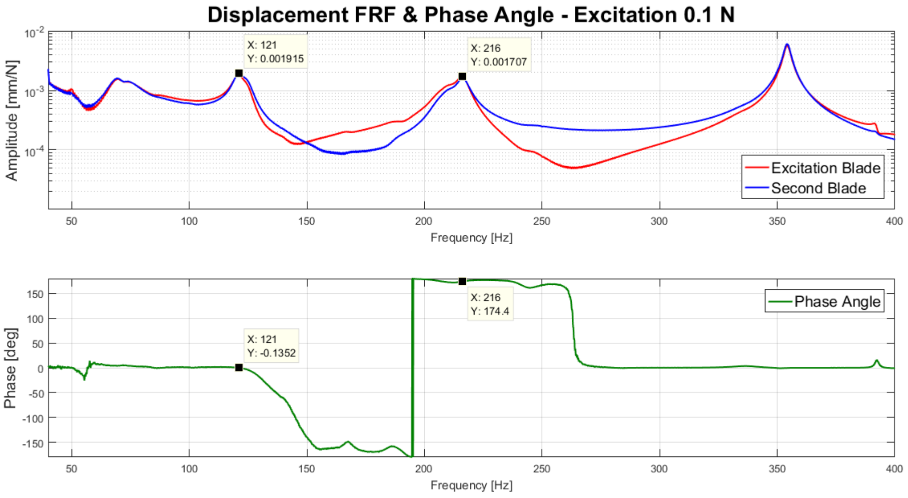

Figure 4.27. Displacement FRFs and Phase Angle of Tip Points of Both Blades in X Direction for 0.1N Excitation

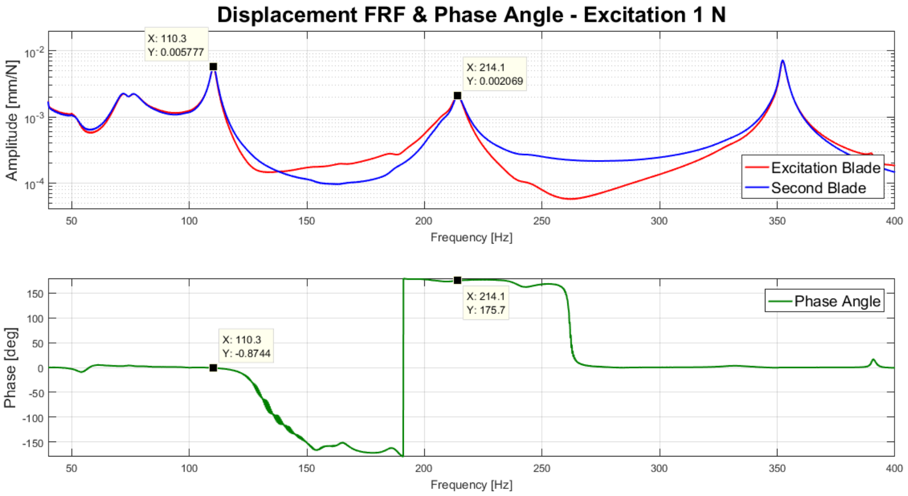

Figure 4.28. Displacement FRFs and Phase Angle of Tip Points of Both Blades in X Direction for 1N Excitation

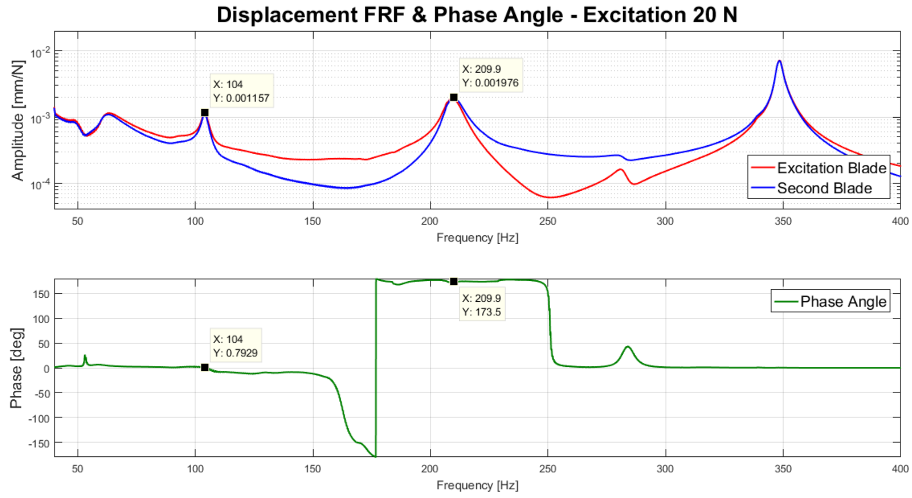

Figure 4.29. Displacement FRFs and Phase Angle of Tip Points of Both Blades in X Direction for 20N Excitation

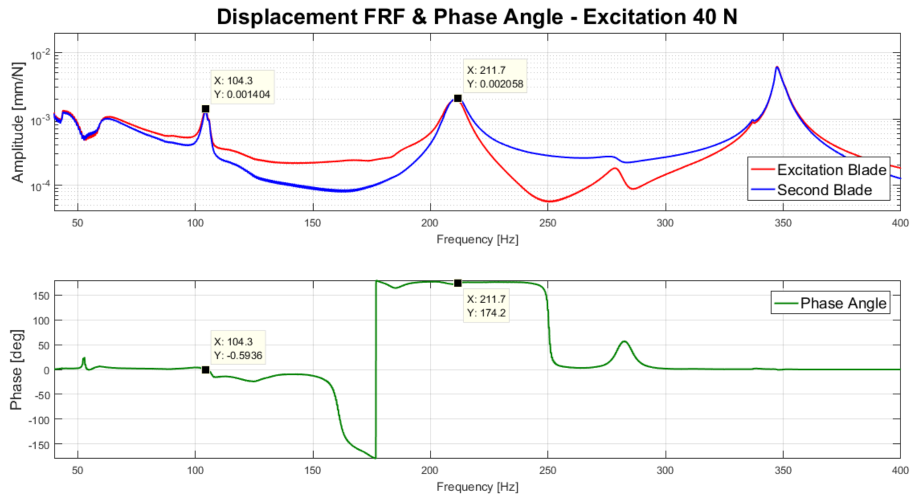

Figure 4.30. Displacement FRFs and Phase Angle of Tip Points of Both Blades in X Direction for 40N Excitation

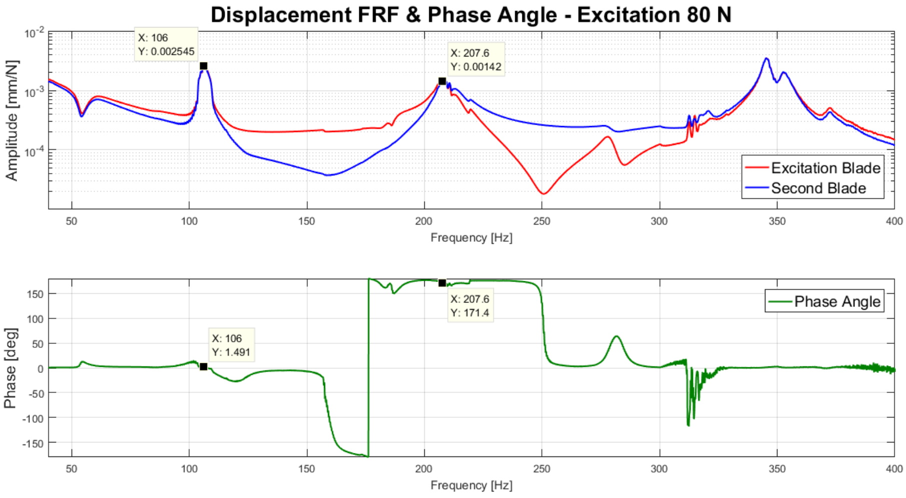

Figure 4.31. Displacement FRFs and Phase Angle of Tip Points of Both Blades in X Direction for 80N Excitation

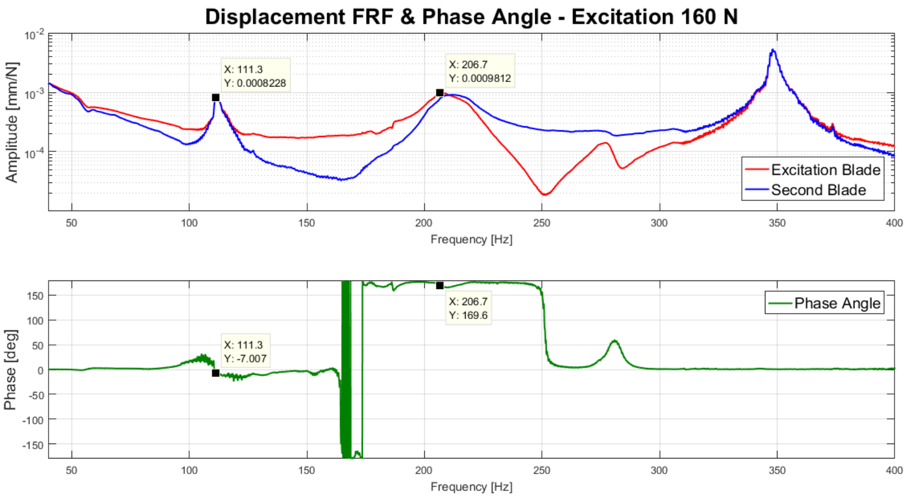

Figure 4.32. Displacement FRFs and Phase Angle of Tip Points of Both Blades in X Direction for 160N Excitation

Inspecting the above figures, it can be concluded that as the excitation amplitude increases IP and OoP mode natural frequencies decreases which is the similar situation in the analysis results. When the preload is kept constant, with the increasing excitation force the system behaves softer as in the case of low contact stiffness scenario obtained in the analysis results. Natural frequencies for IP and OoP modes obtained during the tests for different excitation amplitudes are tabulated in *Table 4.3*

Table 4.3. *Test Results for IP & OoP Modes – Effect of Excitation Force*

UPD Test Results				
Scenario	**Excitation Force**	**Normal Load**	**In-Phase Mode**	**Out-of-Phase Mode**
	[N]	**[N]**	**[Hz]**	**[Hz]**
1	-	Fixed (Glued)	213.0	234.5
2	0.1	44	121.0	216.0
3	1	44	110.3	214.1
4	20	44	104.0	209.9
5	40	44	104.3	211.7
6	80	44	106.0	207.6
7	160	44	111.3	206.7

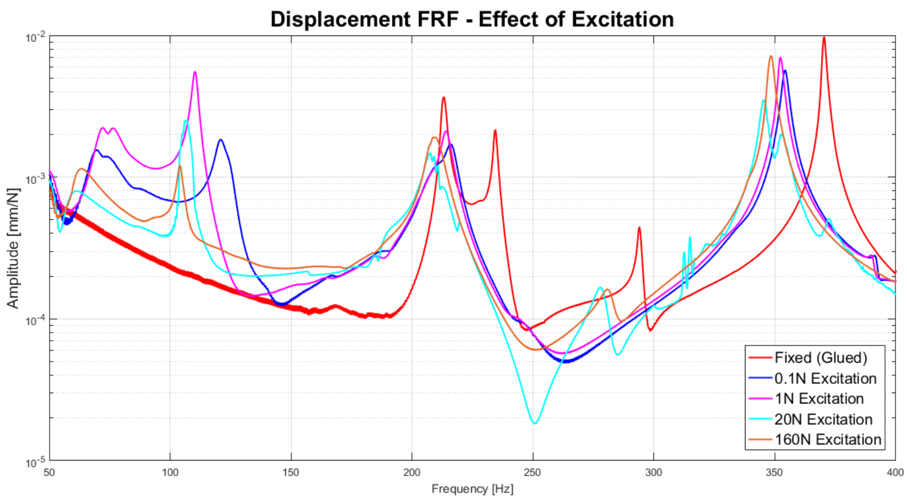

Figure 4.33. Effect of Excitation Amplitude on IP and OoP Experimental Responses

Figure 4.33 shows the normalized displacement FRFs for four different excitation amplitudes together with the fixed UPD case. It can be concluded that the sensitive region lies between the 1st and 2nd scenario. In order to obtain more responses at the intermediate region the excitation force has to be lowered, however below 0.1N the noise floor of the sensor is reached and hence further tests could not be conducted. By using a lower range impedance head these results can be obtained.

The IP and OoP time domain responses are also investigated in order to observe the time domain responses of the blade tip points at these specific frequencies, a 4th order Butterworth bandpass filter is applied. Forward and backward filtering is applied in order to prevent the phase shift on the data due to filtering. 1st test scenario is selected for illustration purposes of the time domain responses. Unfiltered and filtered time domain responses of both blades' tip points are shown in Figure 4.34 for both IP and OoP responses. Only a few seconds of the time domain response extracted with filtering since the excitation is sweep sine. Hence, this part of data contains IP mode frequencies which is between 210 and 216 Hz; and between 232 and 237Hz for OoP mode respectively.

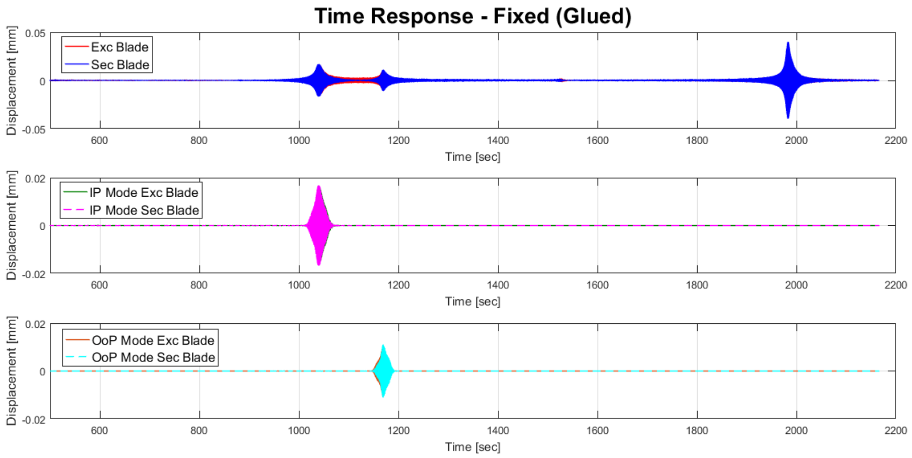

Figure 4.34. Unfiltered and Filtered In-Phase and Out of Phase Displacement Responses of both Excitation and Second Blade Tip Points

Additionally, zoomed in time domain responses are presented in Figure 4.35 for both IP and OoP responses.

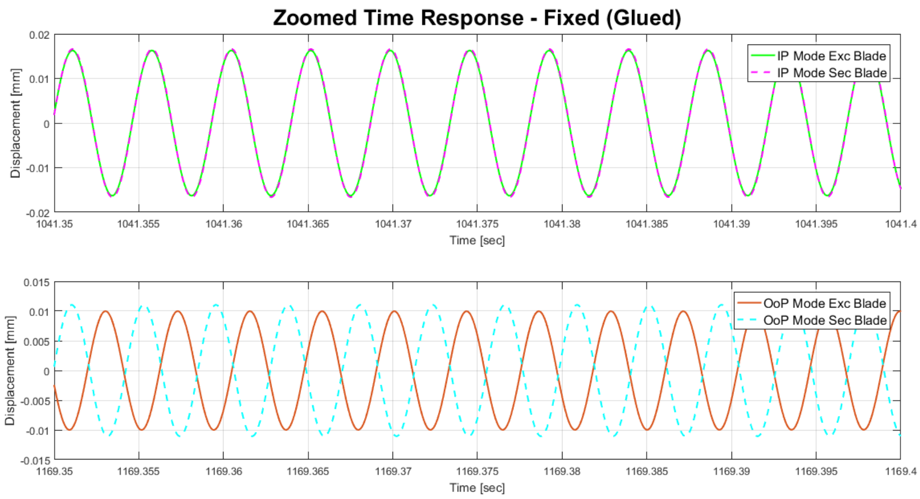

Figure 4.35. Zoomed in IP and OoP Displacement Responses of Tip Points

It can clearly be seen from excitation and second blade responses are in phase at 213Hz and out of phase at 234.5 Hz.

4.2.2. Effect of Normal Load at the Contact Interface

After observing the effect of excitation amplitudes, the effect of normal load is also investigated. Five different normal loads are applied at the contact interface by changing the dead weight hanged at the leverage system. The results are given in Figure 4.36 and the zoomed in graphs for IP and OoP modes are given in Figure 4.37.

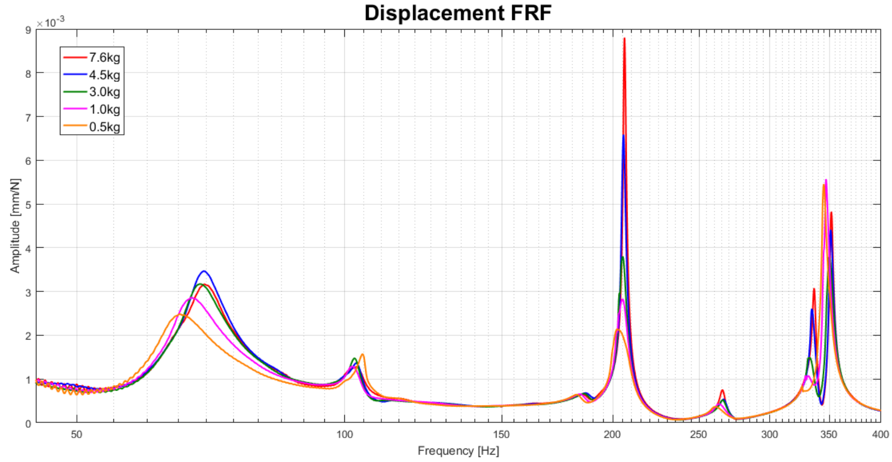

Figure 4.36. The Effect of Normal Preload on Displacement FRF

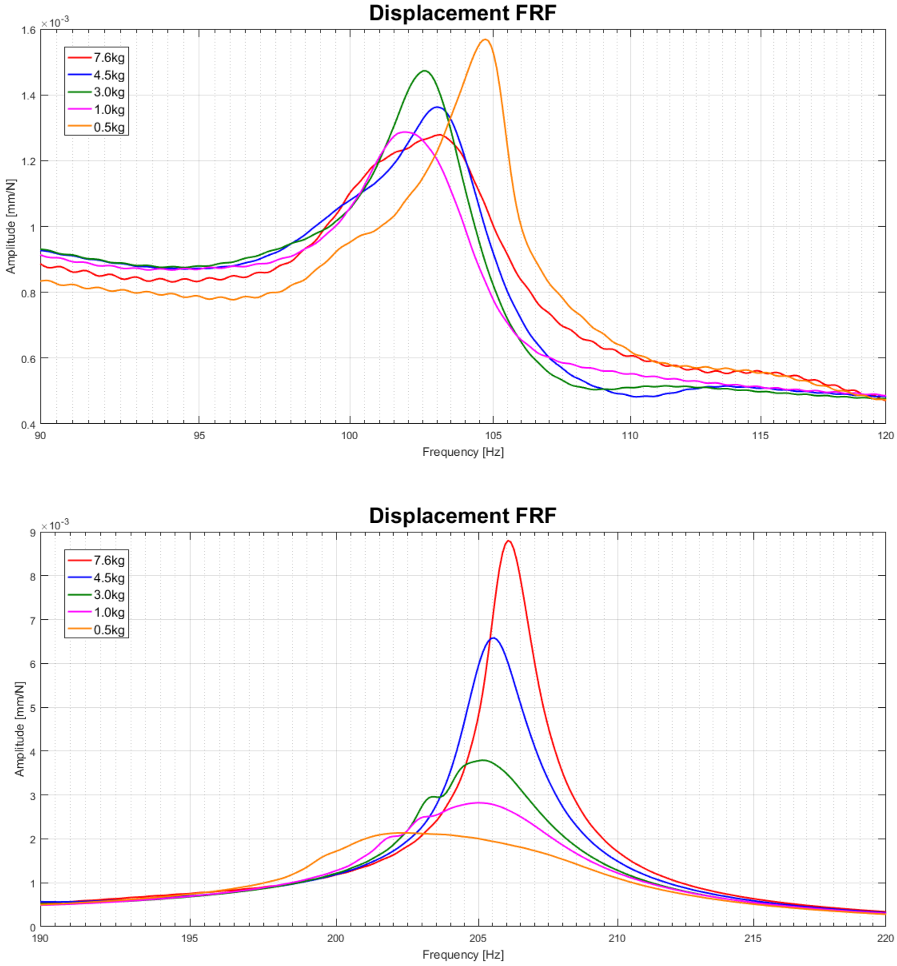

Figure 4.37. Zoomed in IP and OoP Displacement Responses of Tip Points

It can be seen from the above figures that as the normal preload decreases the OoP mode frequency decreases which are in agreement with the simulation results. In the simulations, it was concluded that as the contact stiffness decreases at the interface the resonance frequencies also decreases. However, normal preloads applied here are not enough to excite systems sensitive region. In order to obtain responses at the sensitive region the normal preload should be increased to shift the IP and OoP modes upwards. It was not possible to apply more preload due to the weight balance limitations. Therefore, by increasing the length of the lever mechanism, more responses can be obtained at the sensitive region and above.

.

CHAPTER 5

CONCLUSION AND FUTURE WORK

As stated in Chapter 1, the aim of this thesis is to provide a design guide for the non-linear experimental analysis under realistic conditions. For this purpose, two different experimental test setups are prepared. Two different nonlinear damping mechanisms which are friction and gap nonlinearity are involved.

In order to analyze the dynamical behavior of the gap nonlinearity, a shrouded blade test setup is prepared and effects of different parameters are investigated. Shroud angle, shroud position, excitation amplitude and amount of initial gap are selected as control parameters and their effects on reduction of tip point vibration amplitudes are investigated.

Another blade vibration damping mechanism which utilizes friction at the shroud contact interface is investigated by designing an under platform damper test setup. Validation of the test setup is made by observing in-phase and out of phase modes together with respective time domain responses by inspecting the phase angle of the accelerometers at the tip points.

As future works, the effect of friction in shrouded blade test setup can be included by applying controlled normal load which can be simulated by dummy weights at the contact interface. Also, by increasing the number of shroud angles and positions, the optimal situation can be determined. For both shrouded blade and under platform damper test setups, the response measurements can be gathered by non-contact laser doppler velocimeter (LDV). Moreover, the effect of surface roughness at the contact interfaces can be analyzed by different material UPD elements. Improving the setups by including more parameter effects may complicate the test procedure, however by conducting well-controlled tests better understanding of the nonlinear effects can be obtained.

REFERENCES

[1] Srinivasan A V. Flutter and resonant vibration characteristics of engine blades. Journal of Engineering for Gas Turbine and Power, 1997, 119:742-775

[2] Mitra, M., Arbor, A., Botto, D., Torino, P., Duca, C., Zucca, S. Arbor, A. Contact parameter identification and model verification for a blade-like experimental beam with a large frictional contact, 1(c), 1–3

[3] Berruti, T., Filippi, S., Goglio, L., Gola, M. M., & Salvano, S. (2002). A Test Rig for Frictionally Damped Bladed Segments. Journal of Engineering for Gas Turbines and Power, 124(2), 388. https://doi.org/10.1115/1.1419015

[4] D'Ambrosio, F., Chatelet, E., Ravoux, J., & Jacquet-Richardet, G. (2004). Forced Response of Shrouded Bladed Disc Assemblies: A Jointed Experimental Numerical Approach.

[5] Griffin J H. Friction damping of resonant stresses in gas turbine engine airfoils. Journal of Engineering for Power, 1980, 102:329-333

[6] Szwedowicz J, Kissel M, Ravindra B, et al. Estimation of contact stiffness and its role in the design of a friction damper. Proceeding of ASME Turbo Expo 2001, 2001.7, New Orleans, 2001-GT-0290

[7] Panning L. Sextro W. Popp K.: 2000, Optimisation of interblade friction damper design. Proc. Of the 2000 ASME Turbo Expo, Munich, Germany, ASME Paper GT-2000- 541.

[8] Kaptan, F., Panning-Von Scheidt, L., Wallaschek, J. and Salit, V. (2016). FORCED RESPONSE OF SHROUDED BLADES WITH VARIABLE OPERATING POINTS. Proceedings of the VII European Congress on Computational Methods in Applied Sciences and Engineering (ECCOMAS Congress 2016).

[9] Sanliturk, K. Y., Ewins, D. J., & Stanbridge, A. B. (2001). Underplatform Dampers for Turbine Blades: Theoretical Modeling, Analysis, and Comparison With Experimental Data. Journal of Engineering for Gas Turbines and Power, 123(4), 919. doi:10.1115/1.1385830

[10] Sever, I. A. (2004). Experimental validation of turbomachinery blade vibration predictions, 264. https://doi.org/10.13140/RG.2.1.2497.6883

[11] Firrone, C. M. (2009). Measurement of the kinematics of two underplatform dampers with different geometry and comparison with numerical simulation. Journal of Sound and Vibration, 323(1-2), 313-333. doi:10.1016/j.jsv.2008.12.019

[12] Semenova, I., Sazhenkov, N., Nikhamkin, M., & Semenov, S. (2016). The Numerical Technique for Turbine Blades and Underplatform Dampers Interaction Modeling Based on Substructure Method. Volume 9: Mechanics of Solids, Structures and Fluids; NDE, Diagnosis, and Prognosis. doi:10.1115/imece2016-67068

[13] Botto, D. and Umer, M. (2018). A novel test rig to investigate under-platform damper dynamics. Mechanical Systems and Signal Processing, 100, pp.344-359.

[14] Pesaresi, L., Armand, J., Schwingshackl, C., Salles, L. and Wong, C. (2018). An advanced underplatform damper modelling approach based on a microslip contact model. Journal of Sound and Vibration, 436, pp.327-340.